Check for updates

Original research article

SCIENCE PROGRESS

Science Progress
Vol. 109(3): 1–25
© The Author(s) 2026
Article reuse guidelines:
sagepub.com/journals-permissions
DOI: 10.1177/00368504261466980
journals.sagepub.com/home/sci
Sage

Rapid localization and predictive monitoring of bolt loosening in complex electromechanical systems: Smart washer system based on neural networks

Zhong Tang[1], Jianpeng Jing[1], Liquan Tian[2], Liyun Lao[3], Lulu Yuan[1], and Bangzhui Wang[1]

Abstract

Bolt connections are critical components in combine harvesters, yet they are prone to loosening and failure due to prolonged cyclic vibrations and impact loads. To address the inefficiency of manual inspections, this study proposes a rapid detection method and an intelligent monitoring system for bolt groups. First, a novel detection method based on piezoresistive sensors and a series resistance circuit is introduced, utilizing a unique resistance encoding strategy and a regional binary search mechanism. Second, to enable predictive maintenance, a feedforward neural network model is developed to forecast bolt pressure trends based on historical data. Furthermore, an intelligent monitoring washer is designed, featuring LoRa wireless communication and integrated miniature solar panels. Experimental evaluations show that this approach improves detection efficiency by up to 91.7%-operationalized as the reduction in required inspection steps-compared to traditional sequential methods. The developed feedforward neural network achieved prediction errors within 5%. Finally, the entire system is integrated into a Python-based visual platform for real-time data acquisition, trend analysis, and loosening warnings. This research provides a robust engineering solution for the online monitoring and health management of agricultural machinery.

Keywords

bolt loosening, combine harvester, piezoresistive sensor, resistance circuit, neural network, smart washer

Received: 30 December 2025; Revised: 2 June 2026; Accepted: 23 June 2026

1. Introduction

As one of the most commonly used standardized connection methods in mechanical engineering, bolt connections play an irreplaceable and vital role in large agricultural machinery such as combine harvesters. Their advantages include simple

[1]College of Agricultural Engineering, Jiangsu University, Zhenjiang, China
[2]Intelligent Manufacturing College, Jinhua University of Vocational Technology, Jinhua, China
[3]Faculty of Engineering and Applied Sciences, Cranfield University, Cranfield, UK

Corresponding authors:
Zhong Tang, College of Agricultural Engineering, Jiangsu University, Xuefu Road, Zhenjiang 212013, China.
Email: zht@ujs.edu.cn

Liquan Tian, Intelligent Manufacturing College, Jinhua University of Vocational Technology, Huaotan West Road, Jinhua 321017, China.
Email: tlqbuct@foxmail.com

Liyun Lao, Faculty of Engineering and Applied Sciences, Cranfield University, College Road, Cranfield MK43 0AL, UK.
Email: l.lao@cranfield.ac.uk

Creative Commons Non Commercial CC BY-NC: This article is distributed under the terms of the Creative Commons Attribution-NonCommercial 4.0 License (https://creativecommons.org/licenses/by-nc/4.0/) which permits non-commercial use, reproduction and distribution of the work without further permission provided the original work is attributed as specified on the SAGE and Open Access pages (https://us.sagepub.com/en-us/nam/open-access-at-sage).

structural design, ease of installation, and a high degree of standardization, making them particularly suitable for modular assembly and frequent maintenance of vulnerable components in agricultural machinery systems.

Traditional maintenance of bolts in agricultural equipment relies heavily on manual inspections, which are inefficient and often fail to detect loosening at an early stage. Given the large number of bolt connection points in equipment like combine harvesters, there is an urgent need to develop intelligent monitoring systems capable of efficient identification, real-time response, and predictive warning.[1,2] However, the working environment of agricultural machinery is complex. Equipment such as combine harvesters is subjected to multiple sources of stress-including engine torsional vibration, threshing impacts, sieve body disturbances, and terrain-induced jolts-posing significant challenges to bolt integrity. In the field of sensors, existing research has developed a spray coverage and deposition quality online monitoring system based on a leaf moisture sensor, achieving multi-point measurements through wireless sensor technology.[3,4] Another study proposed a grain loss sensor based on the piezoelectric effect and an adaptive neuro-fuzzy inference system. By optimizing the sensitive structure and signal processing circuits, this sensor significantly improved the accuracy and range of grain cleaning loss measurements during combine harvester operation.[5]

In terms of intelligence, recent studies have constructed a transpiration rate prediction model for greenhouse tomatoes using the CARS algorithm and t-SNE feature interval partitioning, providing intelligent decision-making support for precision irrigation control.[6,7] Using the short time Fourier transform for feature extraction and classifier optimization.[8] The challenge of extracting interpretable insights from complex systems has spurred novel approaches, including a unified biological network learning framework and a contextual transparency method for automated decision-making.[9,10] Recent studies have integrated generative AI with object detection, utilizing a LoRA-finetuned Stable Diffusion model to generate high-quality datasets. This approach significantly improved both the precision and recall of the YOLO algorithm in bolt damage recognition.[11] Intelligent monitoring technologies are thus achieving precise perception and decision optimization in structural health diagnostics, bolt condition assessment, and critical equipment monitoring through deep learning, feature extraction, and multimodal sensor fusion-providing smart solutions for the safe operation and maintenance of engineering facilities.

Although bolt loosening does not typically cause catastrophic failures in its early stages, its characteristic of gradual degradation makes bolt connections one of the most easily overlooked yet most common sources of hidden hazards in agricultural machinery. To overcome the 0-60 degree limitation of traditional 2D methods, a 3D point cloud-based approach was developed to accurately measure the full-range bolt loosening angle by analyzing changes in the exposed screw length, achieving an average relative error of 3.46%.[12] Bolt connection safety monitoring technologies are advancing through innovations in structural design optimization, intelligent sensor development, and advanced algorithm implementation.[13,14] Agricultural robotics is being revolutionized through the deep integration of artificial intelligence for autonomous navigation and target detection, enabling fully intelligent, non-destructive human-robot collaboration in complex farming ecosystems.[15,16] By integrating finite element analysis with optimized sensor signal processing circuits and modeling grain distribution behind the cleaning shoe, real-time, high-precision intelligent monitoring of combine harvester grain loss is achieved.[17–19] These technologies are enabling comprehensive condition assessment-from individual bolts to bolt groups-across agricultural machinery, transportation infrastructure, and composite structures, thereby offering systematic solutions for the safe operation and maintenance of engineering systems.

In summary, this study begins with an analysis of connection failure mechanisms and systematically develops a multi-level integrated system tailored for typical bolt group structures in agricultural machinery, particularly combine harvesters, as illustrated in Figure 1. The system offers several advantages, including rapid detection, high identification accuracy, ease of deployment, trend prediction capability, and scalability. These features collectively provide a practical and effective solution for the intelligent operation and maintenance, as well as health management, of bolted connections in agricultural equipment.

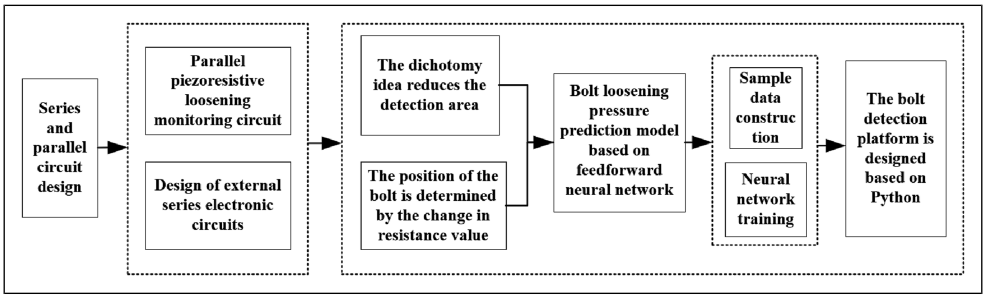

Figure 1. Multi-level integrated system.

2. Materials and methods

2.1 Rapid detection method for loose bolts based on a series resistance circuit

As shown in Figure 2, the bolt loosening monitoring system is based on a series circuit, with its core mechanism relying on the following: each bolt is equipped with a piezoresistive sensor, a relay, and a uniquely valued resistor. When bolt loosening causes the pressure on the sensor to exceed a predefined threshold, a control signal is generated to activate the corresponding relay. Once triggered, the relay closes and short-circuits its associated resistor, thereby altering the total resistance of the series circuit. Because each resistor has a unique value, the change in total resistance directly indicates which bolts have loosened and how many are affected. The relays in the circuit function as switches that respond to threshold signals, automatically opening or closing specific resistance branches.

Once the application of the loosening torque ceases-indicating the bolt has reached its maximum loosened state-the torque value rapidly drops to zero, forming a plateau. The dynamic variation in compressive pressure closely mirrors that of the torque. During the initial phase, the pressure decreases gradually; however, upon reaching a critical loosening point, it plunges sharply toward zero. Although the manual simulation process introduces slight variations in the duration of each phase, a comparative analysis of four independent test sets reveals a highly consistent evolutionary trend. Notably, the data identify a critical inflection point: when the pressure decreases to approximately 78.4 N and the torque simultaneously drops to 0.5 N·m, the loosening process accelerates significantly, manifesting as a precipitous drop in pressure. Consequently, this specific physical state is accurately defined as the critical threshold for bolt loosening.

To ensure that the bolt connection status diagnosis system based on resistance monitoring possesses reliable identification capability, its parameter design must adhere to strict discrimination criteria. This study proposes a systematic set of design principles to theoretically guarantee the accuracy and robustness of the monitoring system.

To ensure the robust operation of the resistor-coded localization system under practical conditions, comprehensive hardware and logical considerations were implemented. Hardware-induced errors are effectively mitigated by utilizing 1% precision metal film resistors with a low temperature coefficient. Because the base resistance is set in the kilo-ohm range, physical interferences such as parasitic wiring resistance, contact resistance, and switching on-resistance account for less than 0.1% of the total resistance, rendering them negligible. Consequently, evaluating the total resistance of the network provides a highly stable measurement baseline.

At the individual identification level, the resistance characteristics of each bolt node must be precisely designed so that a specified displacement induces a distinctly characteristic impedance change. This distinctiveness is reflected in two dimensions: first, the magnitude of change must be significant, the resistance variation caused by loosening of a single bolt must clearly exceed the system's inherent noise level; second, the response characteristics must be unique-bolts at different locations should exhibit differentiated resistance-displacement response curves to avoid similar impedance variation patterns during loosening.

At the combined identification level, the system requires a comprehensive multi-fault coupling analysis mechanism. This entails designing feature decoupling for all possible bolt loosening combinations, focusing on two key issues: one is to

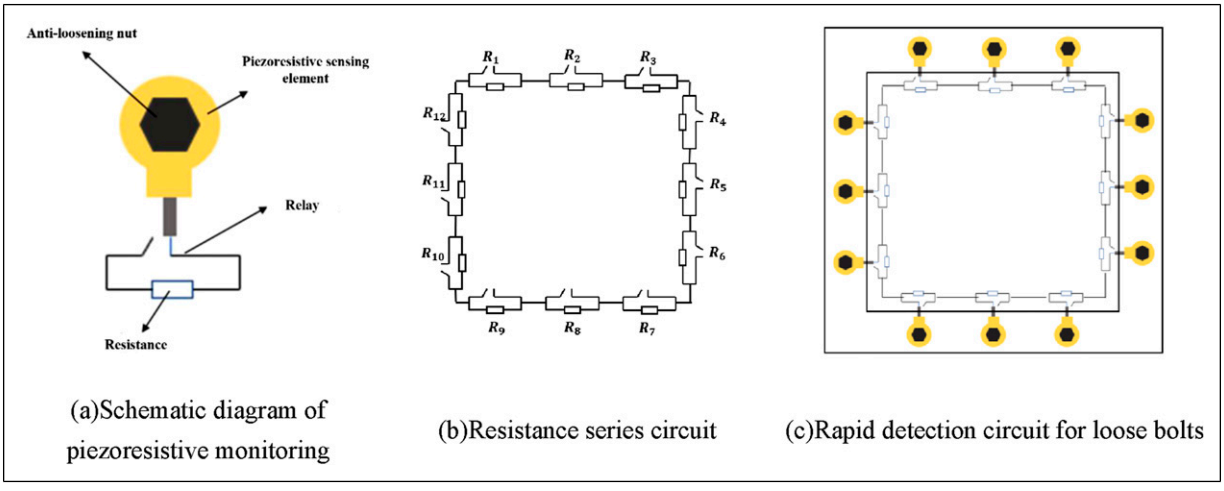

Figure 2. External series resistance loop. (a) Schematic diagram of piezoresistive monitoring. (b) Resistance series circuit. (c) Rapid detection circuit for loose bolts.

eliminate the equivalence between multi-bolt loosening superposition effects and single-bolt faults, ensuring that the overall impedance change for any combined condition is uniquely identifiable; the other is to avoid similar impedance variation magnitudes caused by different bolt combinations, preventing misjudgments by the system. To achieve this, an orthogonal design approach is employed to construct a multidimensional feature space with sufficient discriminative capability.

This dual-constraint mechanism provides a theoretical foundation for bolt connection status monitoring: the individual identification constraint ensures the system's sensitivity to single faults, while the combined identification constraint guarantees diagnostic accuracy under concurrent multi-fault conditions. Through this systematic design approach, common issues such as false alarms and missed detections in traditional monitoring can be effectively overcome, enabling the system to maintain stable performance under complex working conditions. These principles apply not only to agricultural machinery but can also be extended to other engineering scenarios requiring bolt connection status monitoring.

To theoretically guarantee the unique decoding and localization of loosened bolts (injectivity of the condition mapping), this study proposes a binary-weighted resistance encoding strategy. Let a bolt group consist of N bolts. Each bolt i (where i = 1, 2, …, N) is assigned a unique parallel bypass resistor R_i that strictly follows a geometric progression of base 2: $R_i = R_0 \cdot 2^{i-1}$. Where R_0 is the base resistance value. Table 1 presents different loosening scenarios involving five bolts. Assuming R_0 is 1 Ω, the five bolts are assigned discrete resistance values of 1, 2, 4, 8, and 16 Ω, respectively.

A critical challenge in resistance-based monitoring is the susceptibility to measurement noise. To isolate these analog disturbances, this system employs a decoupled electromechanical design. The piezoresistive elements act strictly as threshold triggers; the actual resistance loop consists solely of fixed precision resistors and relay contacts. Consequently, sensor drift and analog noise do not manifest as proportional resistance changes in the monitoring circuit. However, to ensure absolute robustness against environmental temperature fluctuations on the fixed resistors and relay contact resistance

Table 1. Five bolt loosening conditions.

Condition	Quantity of loosening	Number of loose bolts	Whether the regional pressure changes					
			A(1)	B(2)	C(4)	D(8)	E(16)	Data
1	0	None	No	No	No	No	No	No
2	1	A	Yes	No	No	No	No	1
		B	No	Yes	No	No	No	2
		C	No	No	Yes	No	No	4
		D	No	No	No	Yes	No	8
		E	No	No	No	No	Yes	16
		AB	Yes	Yes	No	No	No	3
		AC	Yes	No	Yes	No	No	5
		AD	Yes	No	No	Yes	No	9
		AE	Yes	No	No	No	Yes	17
		BC	No	Yes	Yes	No	No	6
3	2	BD	No	Yes	No	Yes	No	10
		BE	No	Yes	No	No	Yes	18
		CD	No	No	Yes	Yes	No	12
		CE	No	No	Yes	No	Yes	20
		DE	No	No	No	Yes	Yes	24
		ABC	Yes	Yes	Yes	No	No	7
		ABD	Yes	Yes	No	Yes	No	11
		ABE	Yes	Yes	No	No	Yes	19
		ACD	Yes	No	Yes	Yes	No	13
4	3	ACE	Yes	No	Yes	No	Yes	21
		ADE	Yes	No	No	Yes	Yes	25
		BCD	No	Yes	Yes	Yes	No	14
		BCE	No	Yes	Yes	No	Yes	22
		BDE	No	Yes	No	Yes	Yes	26
		CDE	No	No	Yes	Yes	Yes	28
		ABCD	Yes	Yes	Yes	Yes	No	15
		ABCE	Yes	Yes	Yes	No	Yes	23
		ABDE	Yes	Yes	No	Yes	Yes	27
5	4	ACDE	Yes	No	Yes	Yes	Yes	29
		BCDE	No	Yes	Yes	Yes	Yes	30
6	5	ABCDE	Yes	Yes	Yes	Yes	Yes	31

($R_{contact}$), strict error bounds must be established. For unambiguous decoding, the total cumulative noise E_{noise} in the circuit must never cause the measured resistance to bridge the gap to the next discrete state. The mathematical condition for zero-ambiguity decoding is that the absolute measurement error must be strictly less than half of the minimum resolution step (which is R_0): $|E_{noise}| < \frac{R_0}{2}$. If R_0 is selected such that $R_0 \gg R_{contact}$ (for instance, choosing $R_0 = 100\Omega$), the threshold for noise tolerance becomes $\pm 50\Omega$. This provides an exceptionally wide margin for error, ensuring that typical environmental interference (which usually accounts for changes of less than 1 - 2 Ω) will not result in misclassification, thereby guaranteeing high stability in complex combine harvester operating environments.

This encoding scheme perfectly resolves the multiple-loosened-bolts ambiguity. Let the state of bolt i be a Boolean variable $s_i \epsilon \{0, 1\}$, where 1 represents loosened and 0 represents tight. The total change in circuit resistance ΔR caused by any combination of simultaneous multi-bolt loosening is exactly the sum of a binary polynomial: $\Delta R = \sum_{i=1}^{N} s_i \cdot R_0 \cdot 2^{i-1}$. According to the fundamental theorem of binary arithmetic, every integer has a unique binary representation. Therefore, the mapping from the fault location set to the measured resistance change ΔR is strictly injective. The search logic for the system is thus simplified to direct deterministic decoding: dividing the measured ΔR by R_0 and converting the quotient into its binary equivalent directly yields the state matrix of the entire bolt group, isolating exact fault locations without iterative guessing, even in edge cases where all bolts fail simultaneously.

As shown in Figure 3, the X-axis represents discrete combination index numbers ranging from 0 to 31. Each index uniquely identifies a specific bolt combination state. Index 0 corresponds to the baseline state where all bolts are securely tightened, while indices 1 through 31 represent all non-empty combinations in which one or more bolts are loosened. Each enumerated loosening combination index is precisely associated with the specific set of loosened bolts it contains, providing an intuitive reference for subsequent analysis or pattern recognition.

As illustrated in Figure 4, the flowchart depicts a method that assigns a specific resistance value to each bolt in the bolt group and uses the resulting combined resistance changes to uniquely identify which bolts have loosened. The core idea is to establish a one-to-one correspondence between the "loosened bolt combination" and the "total resistance characteristic value".

2.2 Final structural design of the monitoring device

Recent studies have innovatively combined piezoelectric sensor-based ultrasonic monitoring technology with intelligent bolt stress analysis, achieving precise assessment of GIS insulating spacer flange bolt loosening and revealing stress relaxation patterns in industrial pipeline flange connection systems. This dual technological approach provides enhanced safety assurance for power equipment and industrial pipelines.[20,21] Other research proposed a temperature-compensated ultrasonic attenuation model that employs a linear relationship to offset temperature effects on bolt axial force measurements, thereby preventing false alarms caused by temperature fluctuations and improving the reliability of bolt loosening detection.[22] Additionally, serial-parallel multi-sensor technology has been developed, wherein intelligent washers acquire impedance

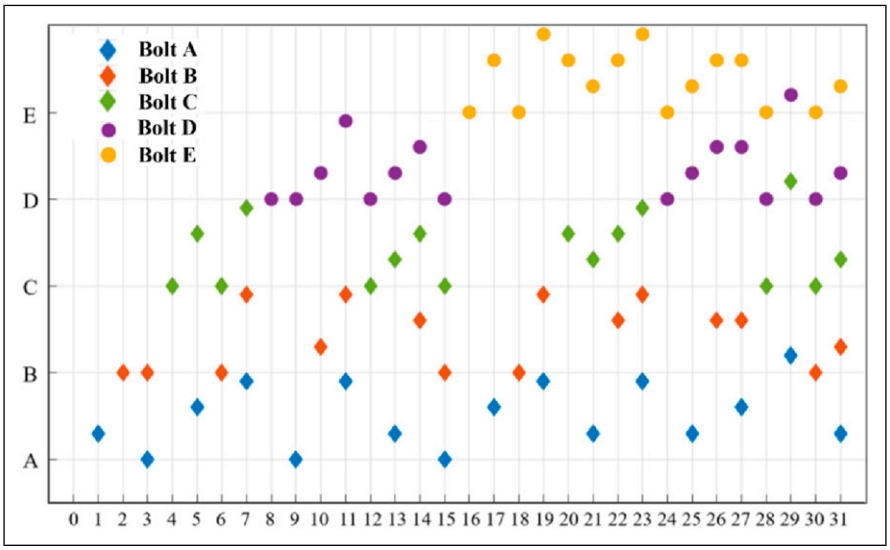

Figure 3. Corresponding combinatorial relationships within the five-bolt system.

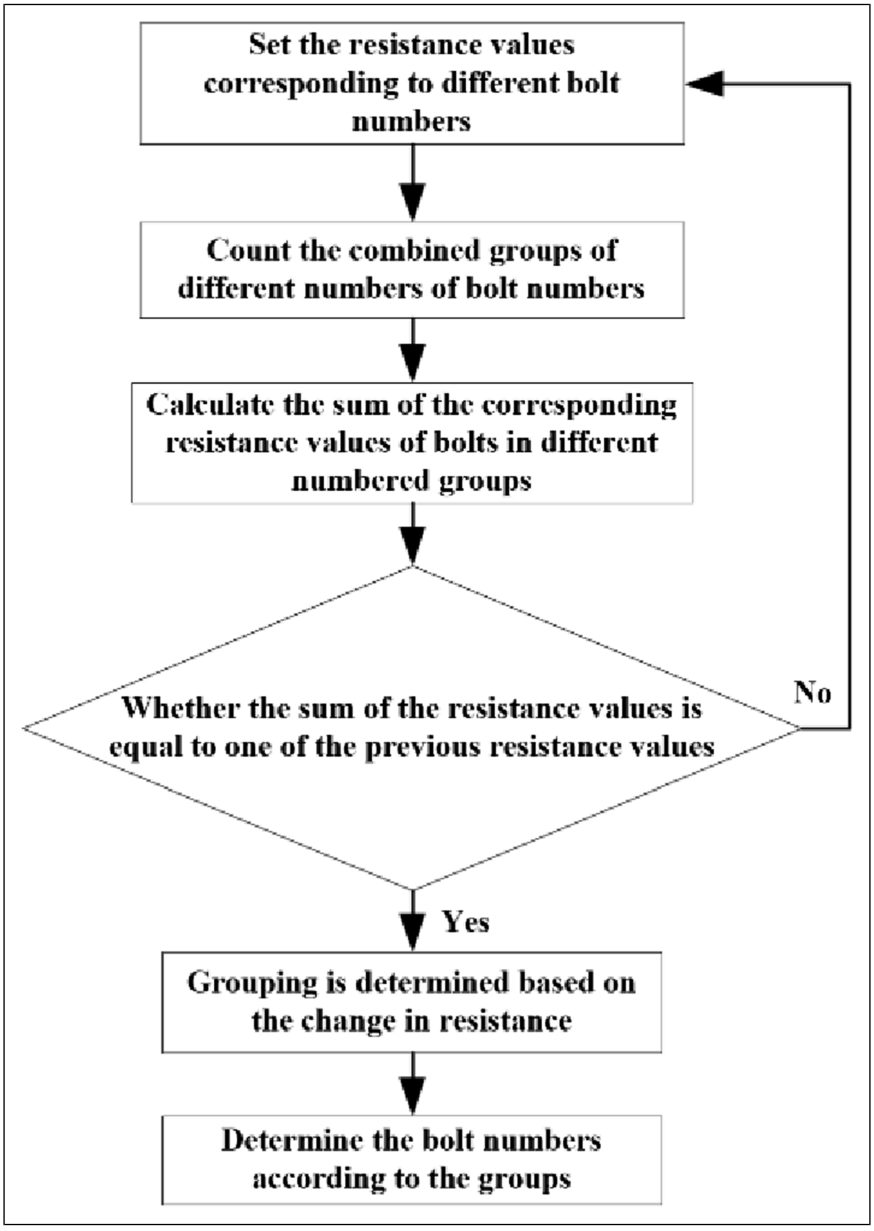

Figure 4. Troubleshooting flowchart for loosening bolts.

signals from bolt groups. Combined with a 3dB bandwidth root mean square deviation algorithm, this method enables loosening localization and severity assessment, offering a novel approach for multi-bolt structural health monitoring.[23] Wave propagation and wavelet energy envelope cross-correlation analyses have also been employed to propose a normalized decorrelation coefficient index for multi-bolt loosening monitoring.[24] Innovative integration of fiber Bragg grating sensors with cam-structure conversion technology has led to the development of an adjustable-range bolt loosening angle sensor system. Through a high-precision angle-to-strain conversion mechanism, this system provides a solution that combines high sensitivity and tunability for large-scale distributed bolt group structural health monitoring.[25,26] The research on intelligent monitoring washers aligns with current key directions in bolt monitoring technology development, emphasizing the use of intelligent signal processing algorithms for precise bolt state identification. This design adopts an innovative structural scheme that maintains the traditional washer functions while achieving an intelligent upgrade in monitoring capabilities. Such a design philosophy continues the pursuit of algorithmic accuracy in bolt loosening detection and achieves breakthroughs in device miniaturization and functional integration, providing a new technological pathway for monitoring connection states in engineering structures.

The core design concept of the intelligent monitoring washer is to integrate complete sensing, processing, communication, and power supply units within the geometric constraints of a standard washer, enabling a plug-and-play bolt status monitoring capability. The overall design follows principles of miniaturization, integration, high reliability, and low power consumption to adapt to the limited installation space and harsh operating environment on combine harvesters.

As shown in Figures 5 and 6, the device is primarily divided into two functional areas:

(1) Preload Force Sensing Component (Front Load-Bearing Section): This part directly bears the axial pressure applied by the bolt head or nut. It contains a core sensing element sensitive to axial force. The external geometry of this sensing component is designed as a ring structure similar to a standard flat washer, featuring a standardized central hole and a smooth annular load contact surface. This design ensures it can seamlessly replace or be stacked within existing bolt connections and effectively transmit the bolt's axial preload force accurately and uniformly to the internal sensing core.

(2) Battery and Circuit Chamber (Rear Functional Integration Section): This area forms a relatively independent, sealed chamber connected to the front sensing component via reliable mechanical and electrical interfaces. Inside this chamber is an integrated set of miniaturized electronics constituting the intelligent core of the device, specifically including:

Signal Acquisition and Conditioning Circuit: Responsible for amplifying, filtering, temperature compensating, and analog-to-digital converting the weak, raw signals from the sensor element into standardized digital data suitable for controller processing. Preliminary analog filtering helps improve the signal-to-noise ratio; however, given the complex and variable strong noise interference in combine harvester environments, more advanced digital signal processing techniques are still required to extract effective loosening feature signals.

Wireless Communication Module: Integrates a low-power wireless transceiver to enable remote data transmission. Considering transmission distance, power consumption, network capacity, and adaptability to complex industrial environments, a low-power wide-area network (LPWAN) technology is preferred. The design aims to ensure reliable signal penetration through the combine harvester's metal structure, cover the entire operational range, and maintain stable communication with a central data collector installed in the cab or other convenient locations.

Microcontroller Unit: A high-performance microprocessor with ultra-low power consumption is selected. Its core tasks include precise control of data acquisition timing, execution of embedded signal processing algorithms, and management of complex wireless communication protocol stacks.

Energy Storage Battery: Ensures the device can operate periodically even without an external power supply.

Integrated Miniature Solar Panel: Embedded on the top surface of the circuit chamber's outer housing, it captures ambient light under illumination conditions and converts it into electrical energy to recharge the internal battery. This design extends the device's autonomous operating cycle and significantly reduces maintenance demands and costs associated with battery replacement.

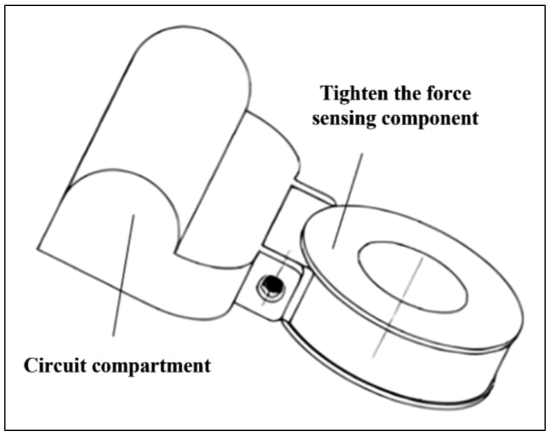

Figure 5. Structural composition of the monitoring device.

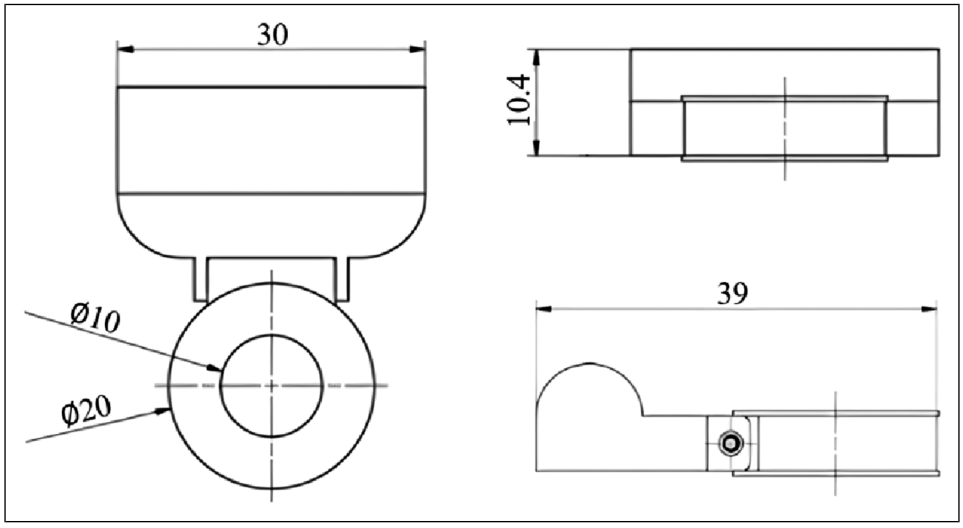

Figure 6. Structure and dimensions of the monitoring device.

2.3 Physical prototype of the monitoring device

Based on the detailed design scheme and technical specifications established above, an intelligent monitoring washer physical prototype was successfully developed by integrating precision machining, high-accuracy injection molding, automated surface-mount technology, as well as final assembly, sealing, and quality control processes. The appearance of the monitoring device prototype is shown in Figure 7.

The key performance indicators of the physical prototype are as follows:

Periodic Autonomous Detection Capability: The device is set to perform detection every 10 minutes. This setting strikes a practical balance between the need for real-time monitoring data and minimizing energy consumption. For the gradual loosening failure process of bolts, a 10-minute data update frequency is sufficient to capture critical trends in preload reduction, enabling early warning.

Long-Distance Wireless Data Transmission: Under standard conditions, the wireless communication range reaches up to 200 meters. This transmission distance allows a single central collector or gateway to effectively cover most areas of a large combine harvester while receiving signals from multiple monitoring washers installed at different bolt locations. As shown in Figure 8, this greatly simplifies the network topology and reduces the complexity of field deployment. Each washer is distinguished by a unique hardware serial number, ensuring data traceability.

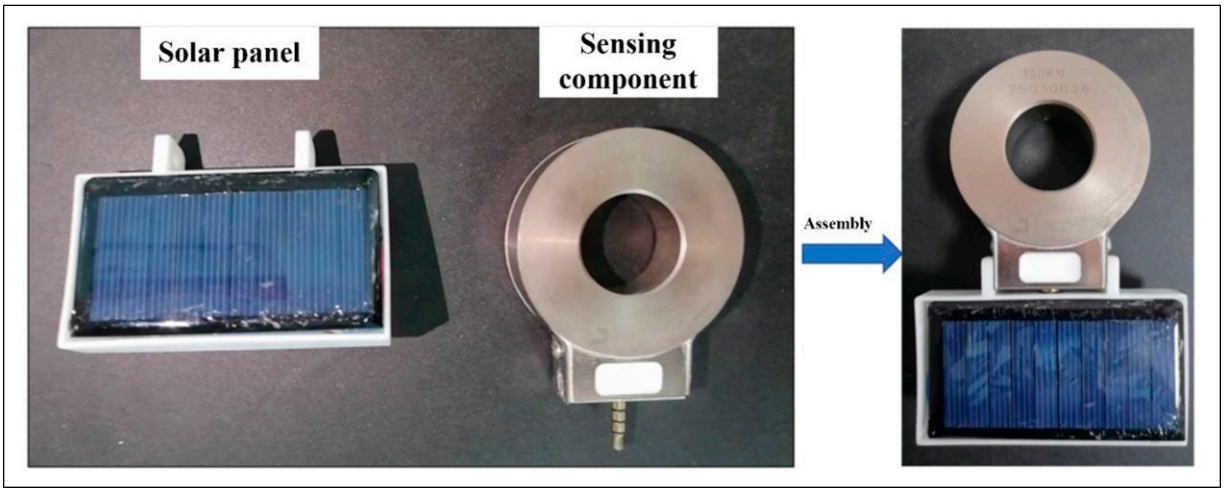

Figure 7. Assembly view of the monitoring device.

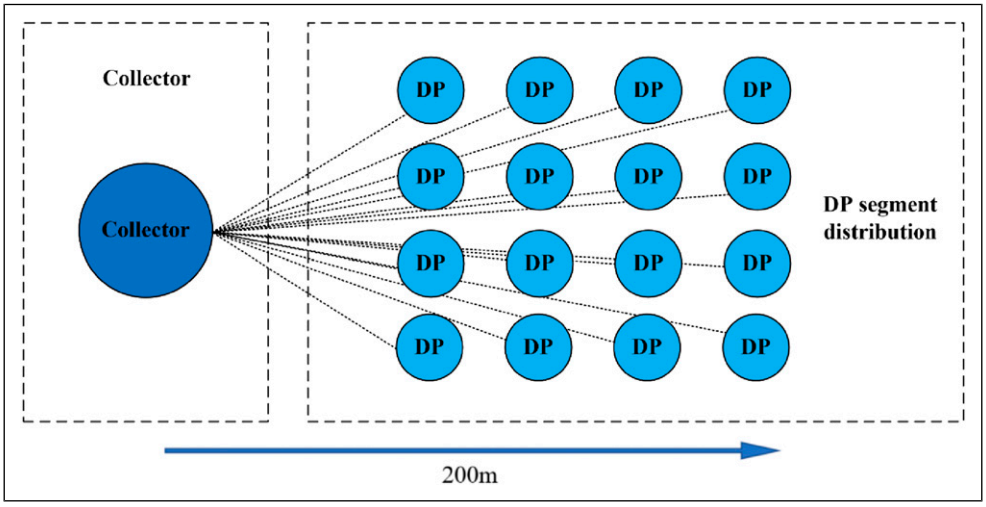

Figure 8. Schematic layout of the collectors and DP terminals.

The system employs a highly reliable power strategy that primarily relies on a built-in lithium battery, supplemented by a miniature solar panel integrated on the top of the device housing. Rather than depending entirely on solar energy, the solar panel serves strictly as an auxiliary power source to harvest ambient light. This approach is underpinned by efficient internal power management and a system-level ultra-low power design, wherein the device operates strictly on a low duty cycle. The node periodically wakes up for data sampling and LoRa transmission, remaining in a micro-ampere sleep state otherwise. Based on a comprehensive evaluation of sleep and peak transmission power consumption, the built-in battery alone is capable of sustaining continuous operation for three months without interruption. This endurance fully covers a typical single harvesting season for agricultural machinery. Ultimately, this robust power design significantly reduces sensor maintenance costs, enhances deployment flexibility for critical monitoring points that are difficult to access after installation, and comprehensively satisfies the practical requirements for long-term maintenance-free operation.

2.4 Integrated design of a bolt loosening early warning system based on intelligent washers

Existing studies have innovatively combined improved wave energy methods with phase-domain impact detection technology, developing a bolt condition monitoring system that integrates contact-based real-time monitoring and non-contact high-precision identification through sinusoidal signal excitation and convolutional neural network analysis, providing a dual assurance solution for structural safety.[27,28] Other research employs piezoelectric sensors coupled with re-mountable devices and artificial neural network data processing to create a low-cost bolt loosening monitoring system that enhances engineering structure safety.[29] To eliminate the reliance on bolt arrangement shapes for perspective transformation; a novel 2D vision method leverages semantic segmentation and corner point extraction to robustly quantify bolt loosening angles with an error of less than 3 degrees.[30] Innovative integration of multitask convolutional neural networks and explainable AI techniques, combined with temperature compensation modules for collaborative feature sensitivity optimization, has enabled lightweight intelligent monitoring models to achieve high-precision recognition of multi-bolt loosening states and torque prediction under limited sample sizes and complex temperature environments.[31–33] Additionally, a multi-bolt loosening identification method based on time-frequency analysis of vibration tonal modulation signals and deep learning, utilizing ResNet-50 networks for intelligent interpretation of time-frequency features, has achieved accurate monitoring of bolt conditions in large steel structures.[34] Another innovative approach combines structural vibration response correlation analysis with deep learning to propose a bolt loosening monitoring model based on the inner product matrix-convolutional autoencoder (IPM-CAE), demonstrating superior recognition accuracy.[35] However, existing research on bolt connection condition monitoring shows clear limitations when applied to the specific context of combine harvesters. As typical large-scale agricultural machinery, combine harvesters have bolt connection systems characterized by large quantities, dense distributions, and harsh operating conditions, making traditional point monitoring methods insufficient for practical engineering needs. Therefore, building on previous technological advances in intelligent sensing and state recognition, this paper proposes an integrated early warning system design for bolt groups in combine harvesters. Through innovative monitoring mechanisms and intelligent analysis algorithms, the system overcomes current technical limitations in

agricultural machinery applications, achieving comprehensive monitoring of bolt fastening conditions and early warning of loosening risks.

Deep learning methods (such as CNN+MLP and multi-stream feature fusion models) typically outperform traditional machine learning methods (like the previously mentioned SVM and Random Forest), as deep learning can automatically learn complex features from raw signals without relying on manual feature extraction. In particular, CNNs can effectively capture local patterns and frequency-domain features in time-series signals through convolutional operations, adapting to the structure of time-series data and possessing strong non-linear modeling capabilities. Meanwhile, the multi-layer structure of deep learning models enables the gradual learning of more abstract features, avoiding the overfitting problems often encountered by traditional methods with high-dimensional data, thereby improving the model's generalization ability and accuracy. Therefore, deep learning methods achieve better classification performance than traditional methods when processing signal data.

The model inputs can be divided into feature inputs and feature result inputs. To reduce computation and improve efficiency, pre-calculated feature results can be used as input, although the raw input method is still retained. Synthesizing the foregoing, the data processing procedure is illustrated in Figure 9. It includes three analysis routes, namely:

① CNN-Driven MLP: Utilizing a Convolutional Neural Network (CNN) to automatically extract features from raw vibration signals, and inputting these features learned by the CNN into a Multilayer Perceptron (MLP) for final classification.
② MLP on Features: This method does not utilize raw signals but relies exclusively on pre-extracted signal features. The vector formed by these features is directly input into a standard Multilayer Perceptron (MLP) network for classification.
③ MLP/CNN Multi-Stream Feature Fusion (MSFF): Combining the strengths of the previous two methods, this approach processes raw signals and signal features simultaneously. It comprises two parallel processing "streams": a CNN stream

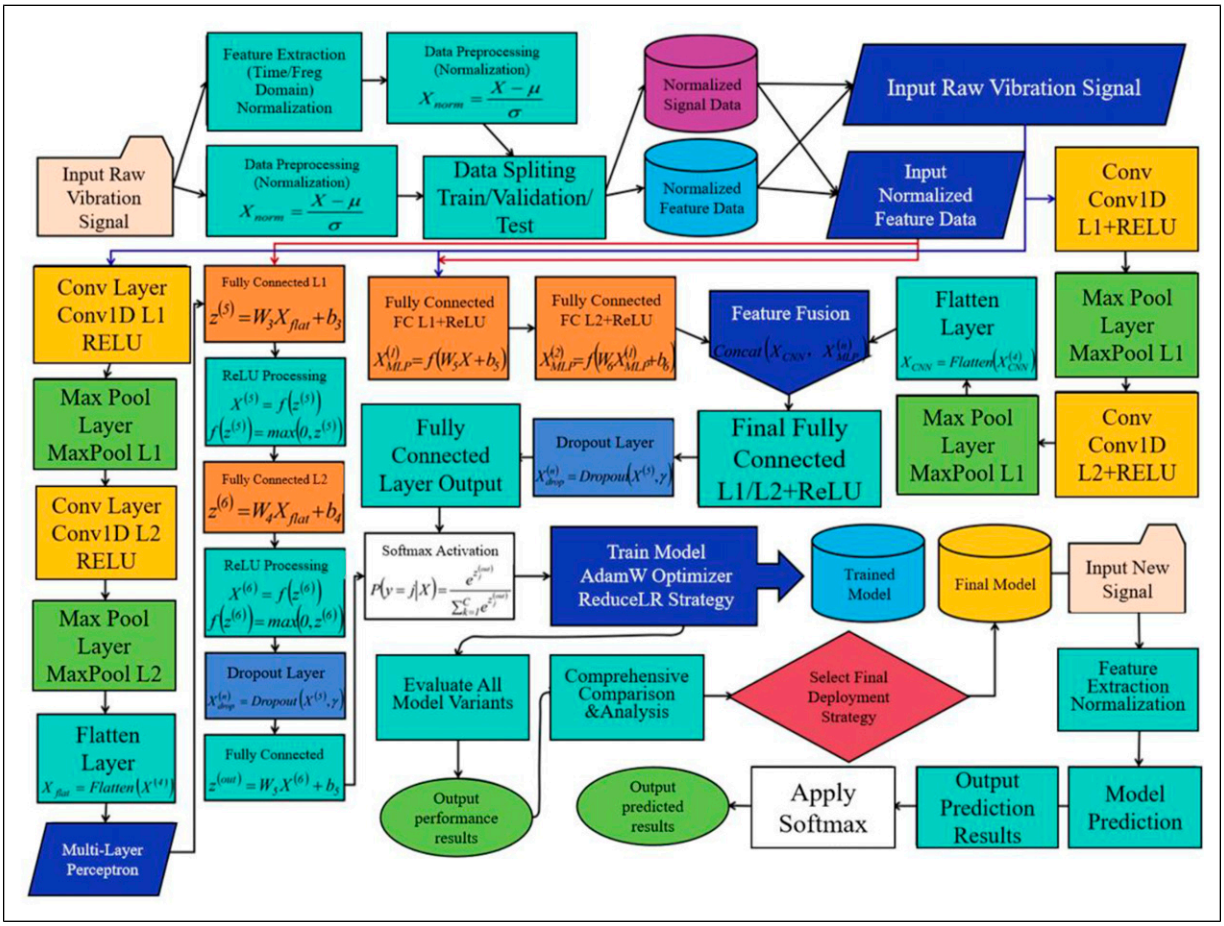

Figure 9. Overall process method of neural network.

that processes raw signals, and an MLP stream that processes signal features. The features extracted from both streams are then fused, and the fused features are finally fed into the classifier.

The learning process and convergence behavior of the three methods-CNN feature-driven MLP, MLP on signal features, and MLP/CNN multi-stream feature fusion are illustrated in Figure 10. The CNN feature-driven MLP model demonstrated highly efficient and exceptional learning capabilities. Over a total of 100 training epochs, the model's validation accuracy rapidly rose to 97% by around the 15th epoch, reached over 98% by approximately the 20th epoch, and maintained this level thereafter. Its validation loss also declined rapidly from an initial 0.74 to 0.25 by the 5th epoch, further optimizing to an extremely low 0.11 by the end of the training.

To construct the neural network dataset and realize the verification of unknown signals, the vibration signals for each of the six operating conditions were extracted into equal-length segments. By allowing a minor degree of overlap, at least 500 signal segments were sampled for each condition. Consequently, the primary data pool for model development consisted of 3,000 vibration signal segments used for training and validation. During the training epochs, forward and backward propagations were executed to update network weights, while a validation subset was continuously monitored via callback functions. If the validation loss stagnated or increased over consecutive epochs, the learning rate was dynamically reduced or early stopping was triggered to prevent overfitting.

Furthermore, to rigorously evaluate the recognition accuracy and strictly ensure the independence of the test data, a completely separate test set was established. Specifically, 6 target vibration signals designated as "unknown signals" were selected from different verification intervals. Using the same sampling method, another 3,000 independent test signal segments (500 segments per condition) were extracted. These 3,000 test cases were completely excluded from the training and validation phases, thereby preventing any data leakage. The test segments were randomly shuffled, and the final classification of the unknown signals was determined by a total confidence voting mechanism across the 500 samples per condition.

The training accuracy of the CNN feature-driven MLP model also steadily increased from 0.62 to 0.9967, and the training loss dropped from 1.503 to 0.0193, indicating that the model achieved a high degree of fit to the training data. In the test set evaluation, the model demonstrated perfect discriminatory capability, with AUC values for all 6 categories, as well as micro-average and macro-average ROC-AUC values, reaching 0.9978. This suggests that the model is capable of distinguishing each category in the test set well from others, with almost no misclassification.

The MLP on Features model is a more traditional machine learning approach that does not process raw signals directly but relies on pre-calculated multidimensional features (time-domain and frequency-domain statistics). The core of the model is a Multilayer Perceptron (MLP) that learns the complex nonlinear relationships between these features and different operating conditions or anomaly categories through fully connected layers. From the training process perspective, this model exhibited extremely high initial accuracy and stable convergence. Across 100 training epochs, its validation accuracy steadily improved from a high starting point of 0.88, finally reaching approximately 0.96 at the end of training. The validation loss also consistently decreased from around 0.5 to a very low level of about 0.1, indicating that the model achieved a good fit on the validation set. Similarly, the training accuracy rose from 0.6389 to 0.9729, and the training loss dropped from 0.9221 to 0.1013. In the test set evaluation, compared with the CNN feature-driven MLP model, this model also achieved commendable classification performance, with AUC values for all 6 categories and micro-average and macro-average ROC-AUC values reaching 0.9846.

The MLP/CNN model exhibited the fastest convergence speed and the lowest final loss among all three models. During the 100 training epochs, its validation accuracy started at approximately 0.60, surpassed 98% within just the first 15 epochs, and finally stabilized at around 99.1%, maintaining a favorable state throughout subsequent training. Concurrently, the validation loss plummeted from an initial value above 1.0 to around 0.1 by the 5th epoch, and was further optimized to approximately 0.05 by the end of training. This is the lowest value among all models, indicating the highest degree of fit on the validation set. The training accuracy also increased from about 0.60 to 99.78, while the training loss decreased from 1.2468 to 0.0017. In the test set evaluation, the AUC values for the 6 categories, as well as the micro-average and macro-average ROC-AUC values, all reached extremely high levels close to 1.00, highlighting the effectiveness of multi-source information fusion.

SHAP (Shapley Additive Explanations) values serve as a tool for interpreting machine learning model predictions. Grounded in the Shapley value theory from game theory, this method assigns an "importance" score to each feature, reflecting the magnitude of its contribution to the model's prediction. To characterize the influence of each feature on the results within the feature data, SHAP values were calculated for both the MLP and the MLP/CNN multi-stream feature fusion methods. For each model, the SHAP value calculation involved extracting one sample from each of the following five categories: misclassified samples, high-confidence samples, low-confidence samples, representative samples, and boundary samples, followed by a feature average calculation. Given a model, the SHAP value of each feature measures its marginal contribution to the model's prediction result. The calculation formula is as follows:

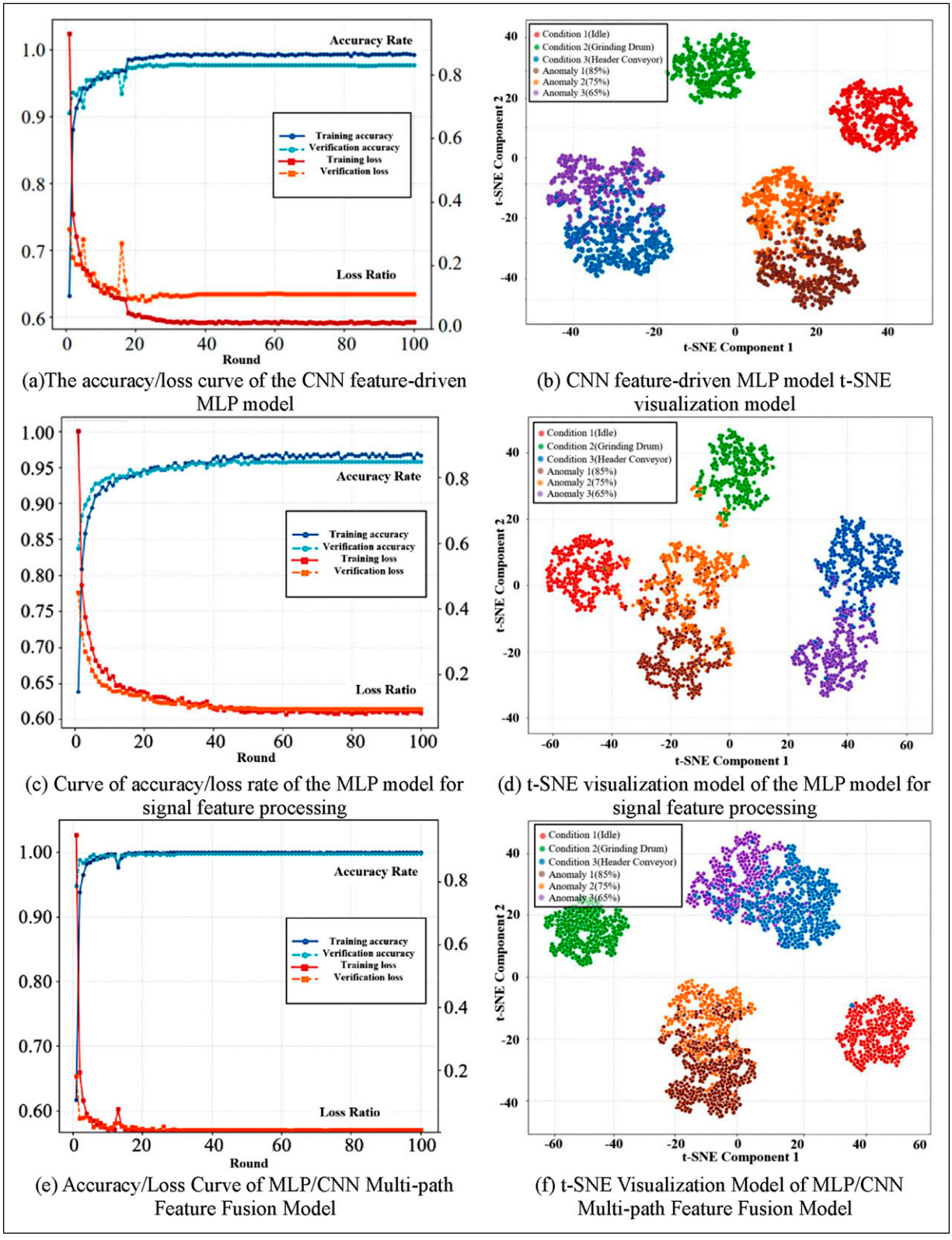

Figure 10. Comparative study of three models of slight loosening signal of conveyor bolt structure. (a) The accuracy/loss curve of the CNN feature-driven MLP model. (b) CNN feature-driven MLP model t-SNE visualization model. (c) Curve of accuracy/loss rate of the MLP model for signal feature processing. (d) t-SNE visualization model of the MLP model for signal feature processing. (e) Accuracy/Loss Curve of the MLP/CNN Multi-path Feature Fusion Model. (f) t-SNE Visualization Model of the MLP/CNN Multi-path Feature Fusion Model.

$$\phi_i(f,x) = \sum_{S \subseteq F \setminus \{i\}} \frac{|S|!(|F|-|S|-1)!}{|F|!} \cdot \left[f_{S \cup \{i\}}(x) - f_S(x) \right] \quad (1)$$

Where F represents the full set of features; S represents a subset of features excluding the feature of interest; $f_s(x)$ is the model output using only features in the subset S; ϕ_i is the SHAP value of the feature. The SHAP value calculation results for the MLP and MLP/CNN multi-stream feature fusion methods are illustrated in Figure 11.

According to the SHAP value analysis of the MLP model, the features the model relies on most are spectral skewness (0.357) and spectral kurtosis (0.324). Additionally, the mean value (0.291), spectral variance (0.253), and bandwidth (0.231) also play significant roles in decision-making. This indicates that when distinguishing between different operating conditions and anomalies, the MLP model primarily judges by analyzing the spectral shape, central tendency, and energy distribution of the signals. Among these core features, the contributions regarding Anomaly 1 (85%) and Condition 3 (header/conveyor) are particularly prominent. Specifically, for spectral skewness, the contribution of Anomaly 1 is 0.102, and that of Condition 3 is 0.081; while for spectral kurtosis, the contribution of Anomaly 1 is 0.093, and that of Condition 3 is 0.071. This suggests that these features are crucial for the precise identification of these two states. In contrast, the contribution degrees for Condition 1 (idling) and Condition 2 (threshing cylinder) across most features are relatively low, all remaining below 0.050. This implies that the MLP monitoring model has relatively low sensitivity in distinguishing these two conditions based on these feature dimensions.

It is evident that frequency-domain features, such as spectral skewness, spectral kurtosis, spectral variance, and bandwidth, occupy a dominant position in the MLP model. This demonstrates that variations in the signal's frequency distribution are key information sources for the model to identify faults and differences in operating conditions. Simultaneously, time-domain features such as the mean value (0.291), Absolute Mean Deviation (AMD, 0.161), and Root Mean Square (RMS, 0.153) also contribute considerably. This indicates that the amplitude characteristics, energy distribution, and fluctuation degree of the signals play an important auxiliary role in the MLP's discrimination of different states.

In the MLP/CNN multi-stream feature fusion model, the model relies most heavily on spectral kurtosis, with a SHAP value reaching as high as 0.485, far exceeding the 0.324 observed in the MLP model. Within this, the contribution of Condition 3 (header/conveyor) to spectral kurtosis reaches 0.183, surpassing even the 0.154 of Anomaly 1 (85%), which demonstrates a

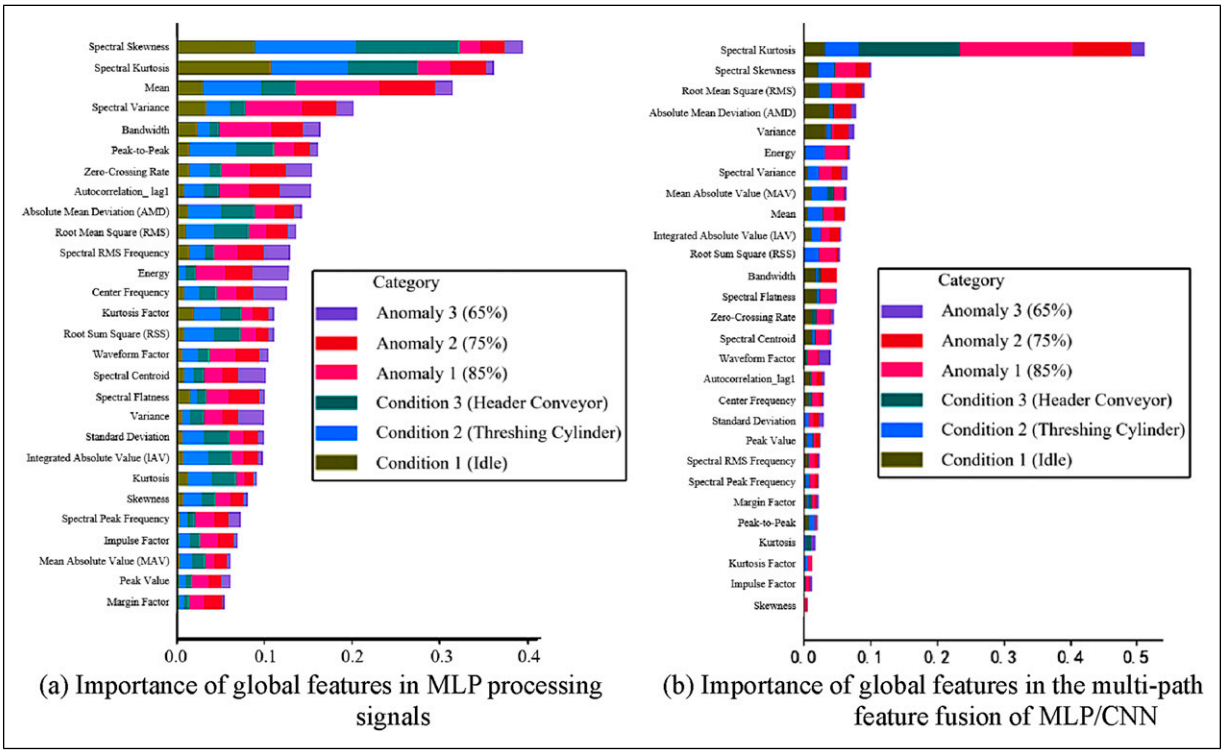

Figure 11. SHAP feature contribution plots for an MLP processing signal features and an MLP/CNN multi-pathway feature fusion model. (a) Importance of global features in MLP processing signals. (b) Importance of global features in the multi-path feature fusion of MLP/CNN.

significant enhancement in the model's ability to identify this operating condition. Spectral skewness, with a SHAP value of approximately 0.211, remains the second most critical feature, where the contribution degrees of both Condition 3 and Anomaly 1 are around 0.05. Compared with the MLP, the MLP/CNN multi-stream feature fusion model significantly weakens the reliance on the majority of original features. For instance, the importance of bandwidth dropped from 0.231 in the MLP to 0.041, energy from 0.144 to 0.083, and mean value from 0.291 to 0.062. This indicates that through deep learning, the model is able to discriminate based on more abstract and refined features, thereby reducing redundant information. Although the contributions of Condition 1 (idling) and Condition 2 (threshing cylinder) across most features remain below 0.030, the model as a whole exhibits a trend of highly concentrating its discriminatory power on a minority of the most effective features.

In this model, frequency-domain features exert greater influence, with spectral kurtosis and spectral skewness being the primary decision factors. This suggests that the model has excavated highly discriminative patterns within the frequency-domain data, while the contribution of time-domain features, such as RMS (0.123) and AMD (0.101), has notably decreased.

3. Results and discussion

3.1 Parallel connection of piezoresistive loosening monitoring devices

The loosening of bolts from installation to failure is a long-term process. In the early service period, only a small number of bolts may loosen. Traditional one-by-one inspection methods are inefficient because, even if most bolts are intact, each bolt still needs to be checked individually. To improve efficiency, a rapid detection method is needed that can quickly identify loosened bolts without inspecting every single one.

To address this issue, the concept of series-parallel electrical circuits can be applied by connecting the monitoring devices together to form a circuit. In this monitoring system, each device acts as a sensing node within the circuit. When any bolt loosens, the electrical characteristics of its corresponding device change, causing a variation in the total resistance or conductance of the entire monitoring circuit. By monitoring these overall circuit parameter changes, it is theoretically possible to quickly locate the specific bolt that has loosened, thereby avoiding the cumbersome process of checking each bolt one by one. The following research is based on this principle and conducts a detailed analysis of a group model containing multiple bolts.

3.1.1 Area monitoring range optimization method based on the bisection principle

Although connecting monitoring devices in parallel can determine whether any bolt in the group has loosened, it cannot quickly identify which specific bolt is loose. To overcome this localization difficulty and improve detection efficiency, this study proposes a divide-and-conquer strategy similar to the bisection method, built upon the parallel network, to systematically narrow the search area and achieve rapid localization.

The core idea is to rapidly localize the target area through iterative regional subdivision. The implementation process includes the following three steps: first, establish a full-area monitoring model based on preset initial parameters; next, apply successive partitioning to divide the monitored region into several subregions; finally, use a parameter feedback mechanism to accurately converge the monitoring range.

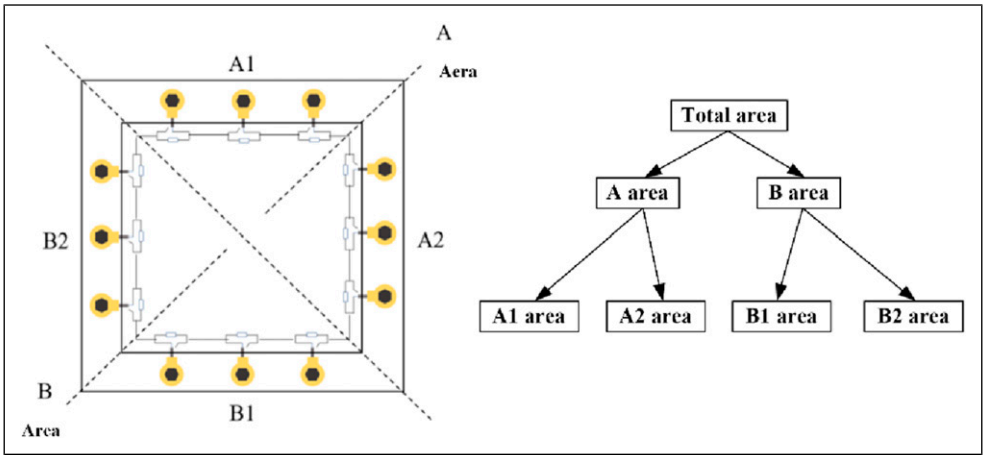

Figure 12. Area monitoring sequence.

Specifically, as shown in Figure 12, the detection region is divided into two subregions, A and B, which are then further subdivided into A1, A2, B1, and B2, and so forth. By applying this bisection concept, the detection range can be quickly narrowed, effectively locating the loosened bolt and improving detection efficiency and accuracy.

As illustrated in Figure 13, this method, combining parallel connection of monitoring devices with the bisection strategy, can be applied in engineering practice, providing a more efficient solution for bolt loosening detection (Table 2).

3.1.2 Comparison with conventional monitoring methods in terms of efficiency

This study systematically validates the technical advantages of the interval segmentation-based monitoring method for fault localization through comparative experimental data presented in Table 3. Five sets of differentiated conditions were constructed to simulate scenarios with varying numbers of loosened bolts, ranging from 0 to 4, with fault locations expanding from single nodes to multi-region compound distributions. The experimental group employed the intelligent partitioned monitoring algorithm proposed in this study, while the control group used the traditional full-area scanning method. Monitoring accuracy was verified via voltage response status.

To adequately operationalize "detection efficiency", this study defines it as the reduction in the number of required inspection steps necessary to fully assess a bolt group, compared to the traditional sequential one-by-one inspection method (Figures 14 and 15). Assuming a bolt group consists of N bolts, the conventional manual method requires N separate inspection steps ($f_1 = N$). In contrast, the proposed binary search method requires f_2 measurements, where f_2 dynamically

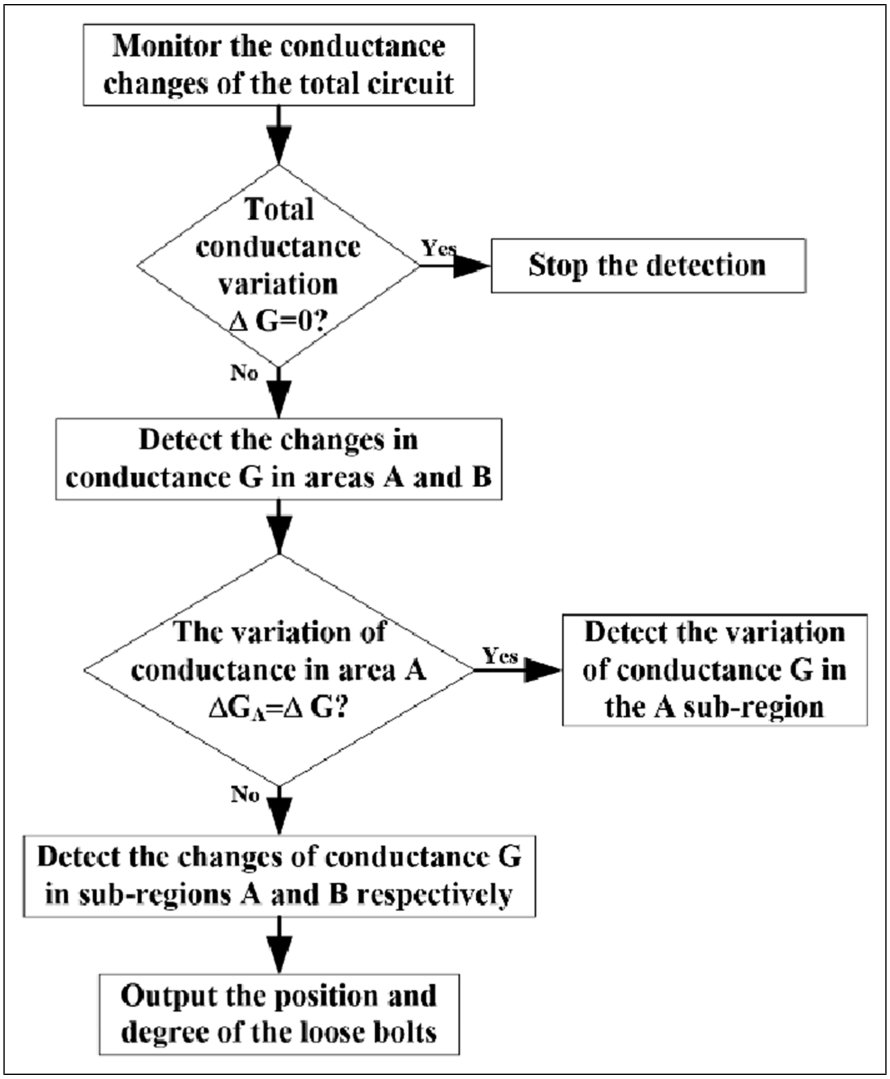

Figure 13. Monitoring technology flow based on dichotomous thought.

Table 2. Performance comparison between the proposed method and traditional monitoring techniques.

Condition	Number of loose bolts	Loose position number	Monitor area voltage response						
			Total area	A area	A1 area	A2 area	B area	B1 area	B2 area
1	0	None	None	None	None	None	None	None	None
2	1	2	Yes	Yes	Yes	None	None	None	None
3	2	1,4	Yes	Yes	Yes	Yes	None	None	None
4	3	3,5,8	Yes	Yes	Yes	Yes	Yes	Yes	None
5	4	1,6,7,11	Yes	Yes	Yes	Yes	Yes	Yes	Yes

adapts based on the number and distribution of the loosened bolts. To quantify this gain, the metric Detection Efficiency Improvement Rate (W) is defined in Equation (2):

$$W = \frac{f_1 - f_2}{f_1} \tag{2}$$

In Equation (2): W represents the efficiency improvement percentage; f_1 denotes the total number of inspection steps required by the standard sequential method (in this 12-bolt system instance, $f_1 = 12$); and f_2 represents the actual number of regional electrical measurements required by the proposed bisection method.

By analyzing Tables 3 and it can be seen that under all five tested conditions (with varying numbers of loosened bolts), the proposed rapid detection method is more efficient than the conventional method. The efficiency improvement is most significant under Condition 1, where no bolts are loosened, reaching 91.7%, since only one inspection is needed to confirm the status. As the number of loosened bolts increases, the efficiency gains decrease correspondingly, with improvements of 75%, 66.7%, 50%, and 41.7%, respectively.

3.2 Feedforward neural network training process and results

To verify the practical performance of the feedforward neural network algorithm, this study utilized denoised sequences from actual bolt loosening measurements. The dataset originated from 30 independent experiments conducted on ten distinct bolts, recording 600 continuous data points per test to comprehensively capture the dynamic temporal evolution of the bolt connection status. To effectively mitigate data redundancy, a systematic sampling method with a 50-point interval was applied. Subsequently, samples were constructed using a sliding window strategy featuring a window size of 8 and a step size of 1. Regarding input features, the model relies exclusively on the raw pressure history. The input dimension was set to 7, directly corresponding to the seven preceding pressure measurements. For the data split strategy, loosening pressure data from the first eight bolts served as the training set, while the complete sequences from the ninth and tenth key bolts were reserved as an independent testing set to rigorously evaluate generalization capability. To prevent overfitting under small sample conditions, a dual regularization mechanism was implemented. This approach incorporated an L2 weight decay with a coefficient of λ=0.01 into the objective function, alongside an early stopping strategy designed to terminate training if the validation set error fails to improve for 15 consecutive iterations. During the evaluation of predictive performance, the model outcomes across different datasets were systematically analyzed utilizing a four-quadrant comparison method. The goodness-of-fit was strictly quantified via the Pearson correlation coefficient, supplemented by a linear regression analysis to

Table 3. Evaluation of Monitoring Instances and Efficiency Improvement: Pre-vs. Post-Scheme Optimization.

Operating conditions	Condition 1	Condition 2	Condition 3	Condition 4	Condition 5
Loosening number	0	1	2	3	4
Loosening bolt serial number	0	2	1,4	3,5,8	1,6,7,11
The number of times required by the standard method f_1	12	12	12	12	12
The number of times required by the proposed method f_2	1	3	4	6	7
Frequency reduction value	11	9	8	6	5
Percentage of efficiency optimization (%)	91.7	75	66.7	50	41.7

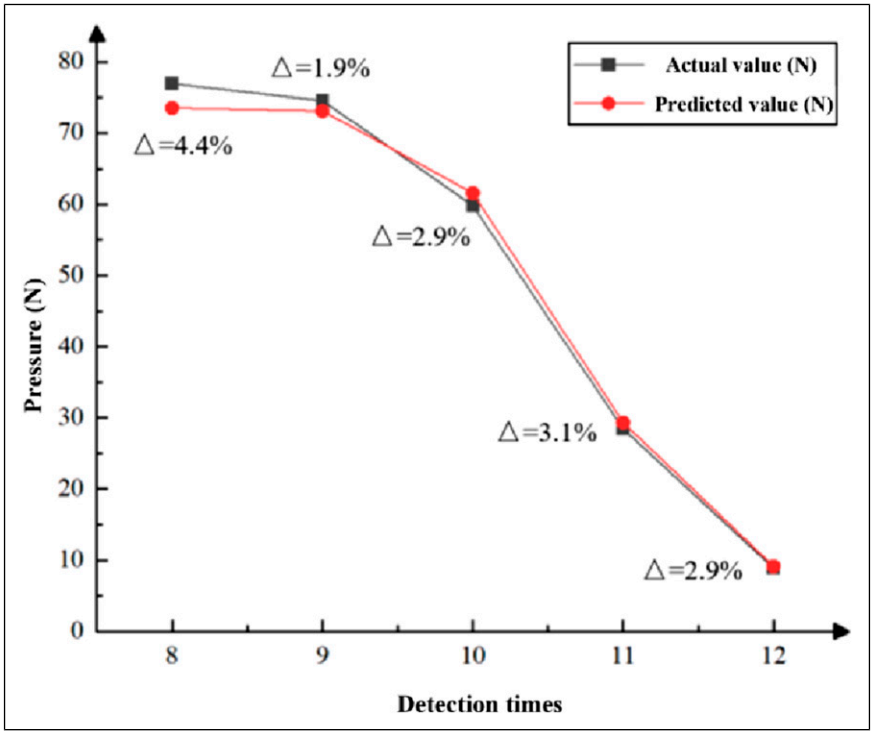

Figure 14. Prediction of loosening time sequence of bolt 9.

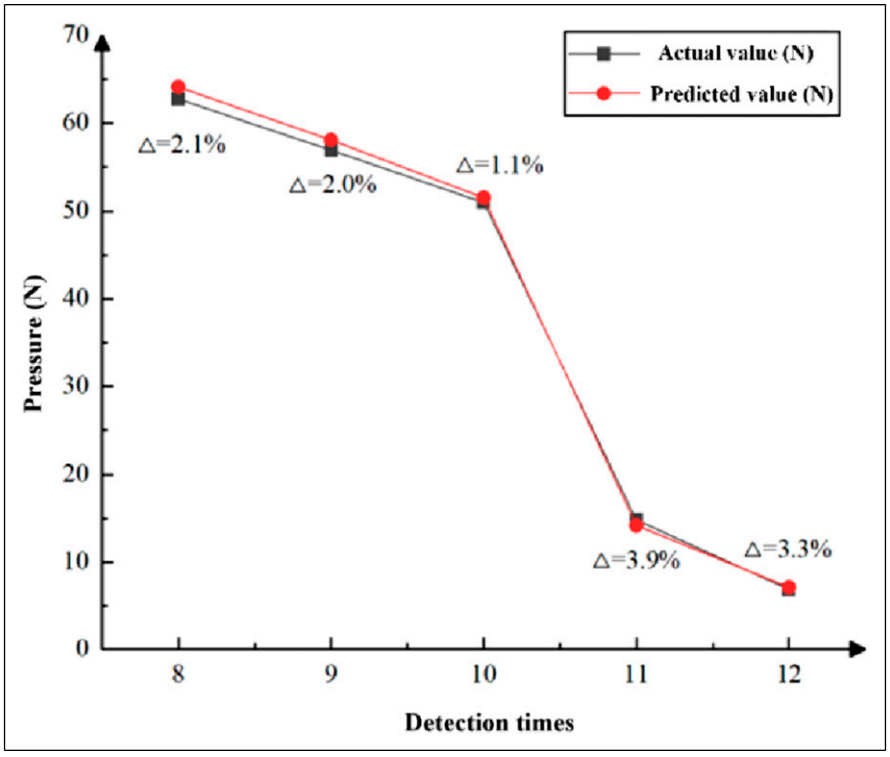

Figure 15. Prediction of loosening time sequence of bolt 10.

elucidate system bias characteristics. The test results demonstrate that the overall trajectory of the predicted sequences, generated based on the preceding seven data points, aligns closely with the actual observations. Furthermore, the prediction errors at specific temporal nodes typically do not exceed 5%.

This study presents the experimental monitoring charts using a multi-axis composite visualization method to systematically demonstrate the dynamic convergence characteristics of the optimization algorithm, comprising three temporally correlated subplots. The vertical axis parameters reveal the evolution of numerical stability throughout the optimization process. As shown in Figure 16, the gradient values exhibit a typical exponential decay trend, reaching the magnitude of 1.2526×10^{-9} by the 6th iteration-about three orders of magnitude lower than the initial value. The gradient curve displays an inflection point between the 3rd and 4th iterations, where the decay rate accelerates, consistent with the superlinear convergence expected from the quasi-Newton method. The Mu value, shown on a double logarithmic scale, exhibits a coordinated decay pattern with the gradient. It remains constant at 1×10^{-6} during the initial phase (iterations 0–2), then enters an adaptive adjustment stage starting from the 3rd iteration, finally stabilizing at the threshold of 1×10^{-8}. The correlation analysis chart, shown in Figure 17, uses a four-quadrant comparison method to systematically present the predictive performance of the machine learning model across different datasets. The plotted matrix represents the mapping relationship between predicted outputs and target values for the training set, validation set, test set, and the entire dataset. Pearson correlation coefficients (R) quantify the model's goodness of fit, supplemented by linear regression analysis to reveal system bias characteristics.

3.3 Performance testing of the monitoring device

After the successful development of the intelligent monitoring gasket prototype, performance verification tests were conducted to comprehensively evaluate the actual performance of the monitoring device. A performance test platform, as shown in Figure 18, was established. This platform is primarily used to verify the core functions of the device, especially its data acquisition capability and the reliability of LoRa wireless data transmission, ensuring that the wireless communication link operates as designed.

To eliminate external environmental disturbances and ensure the repeatability of the baseline verification, all experiments in this study were conducted under a controlled laboratory environment. The ambient temperature was maintained at

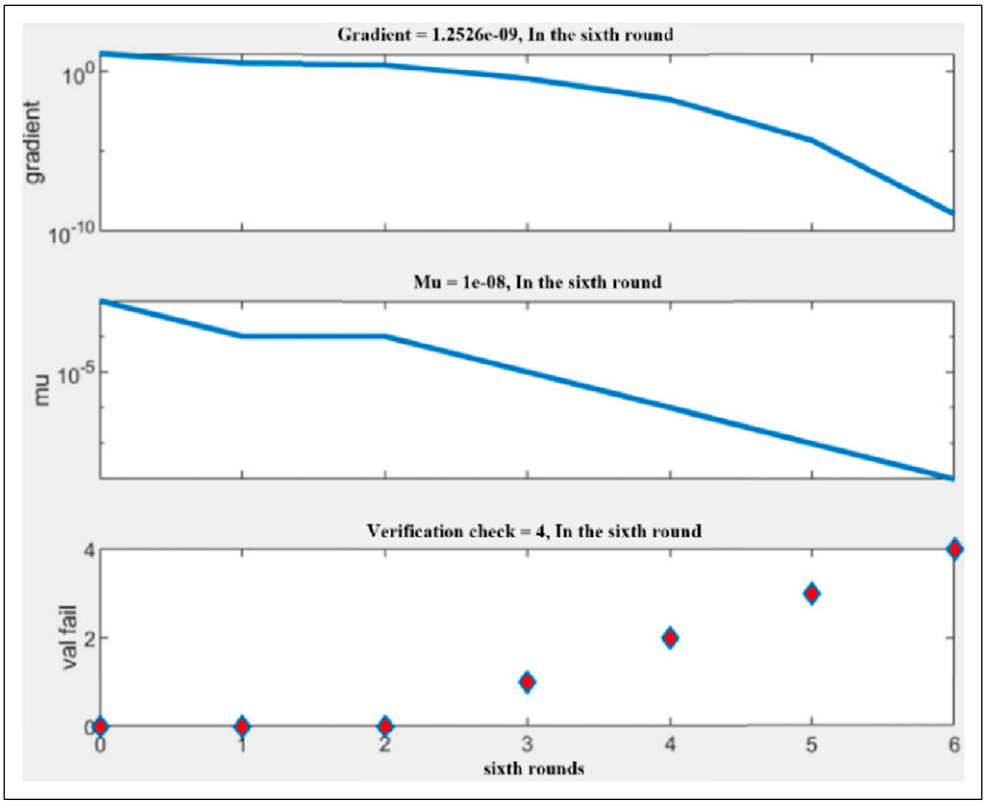

Figure 16. Training state.

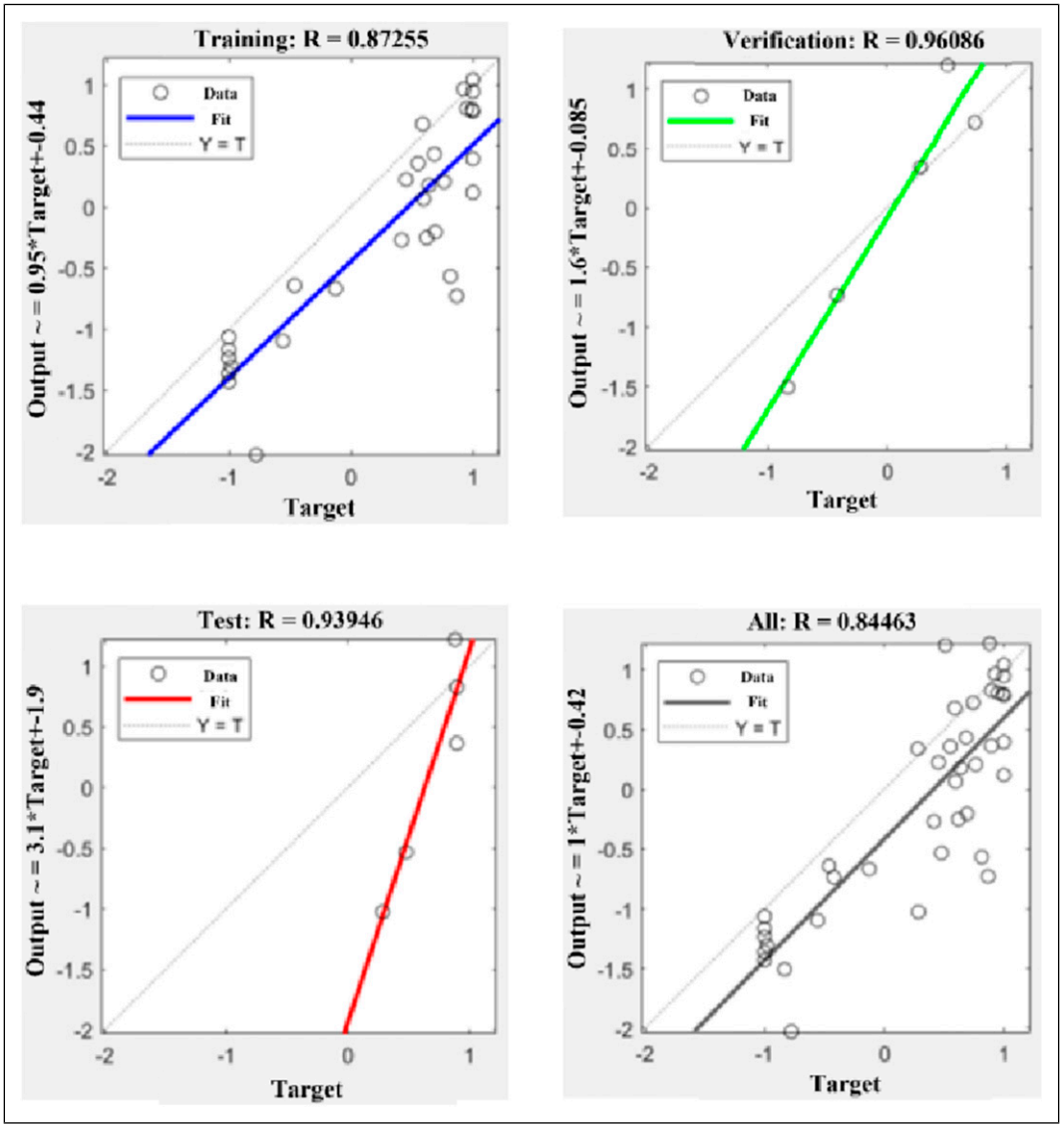

Figure 17. Multi-data set regression performance analysis of bolted joint pressure prediction model.

approximately $25 \pm 2\,^{\circ}C$ with a relative humidity of $45 \pm 5\,\%$, in a dust-free state. Furthermore, the bolt groups were subjected to static and step-loading rather than dynamic long-term cyclic loading.

During the test, a digital torque wrench was used to apply force or torque simultaneously to two sensor elements fixed on the clamping fixture. The sensor elements converted the measured physical quantities into electrical signals and wirelessly transmitted them via the LoRa module. The receiving LoRa module connected to a laptop received the data, which was displayed and recorded in real time using data acquisition software.

The bolt assembly containing the sensor elements was firmly mounted on a bench vise to ensure no shaking or rotation during torque application. The LoRa transmitter was connected to ensure the sensor signals were properly input to the LoRa transmission module. The LoRa receiver was connected to the laptop's USB port via a USB-to-TTL adapter. The data acquisition software on the laptop was started, with the correct COM port and baud rate configured.

Communication was checked to confirm that the laptop software could receive data from the LoRa transmitter. The digital torque wrench was powered on and zeroed. At the start of the test, the bolt was ensured to be fully loosened, and the sensor readings at this initial state were recorded on the computer.

The digital torque wrench was then slowly and steadily applied to the bolt head, increasing torque until the bolt was fully tightened, then slowly loosened back to the initial state. This full tightening and loosening process was repeated twice to evaluate the accuracy of the sensor elements.

Figure 18. Schematic diagram of the monitoring device performance test platform.

Data transmission continuity and accuracy were also monitored to assess key performance indicators of the LoRa module under current conditions, including wireless transmission range, reliability, and real-time performance.

As shown in Figure 19, the real-time data display interface of the mechanical monitoring module intuitively presents the dynamic process of bolt pressure changes during torque application and release over two repeated experiments. The blue and red curves correspond to the two measurements, and their similar shapes directly reflect the repeatability of the measurements. Meanwhile, the data communication section below provides detailed records of the raw data. Through this interface, users can monitor bolt pressure changes in real time and obtain both raw and visualized data for subsequent analysis.

Figure 20 presents a comparison of the pressure characteristics of two bolts during the torque loading process based on two independent tests. The graph clearly illustrates the increase of the preload force throughout the loading process and reveals possible differences under varying test conditions in terms of the rate of preload increase, the final achieved value, and the

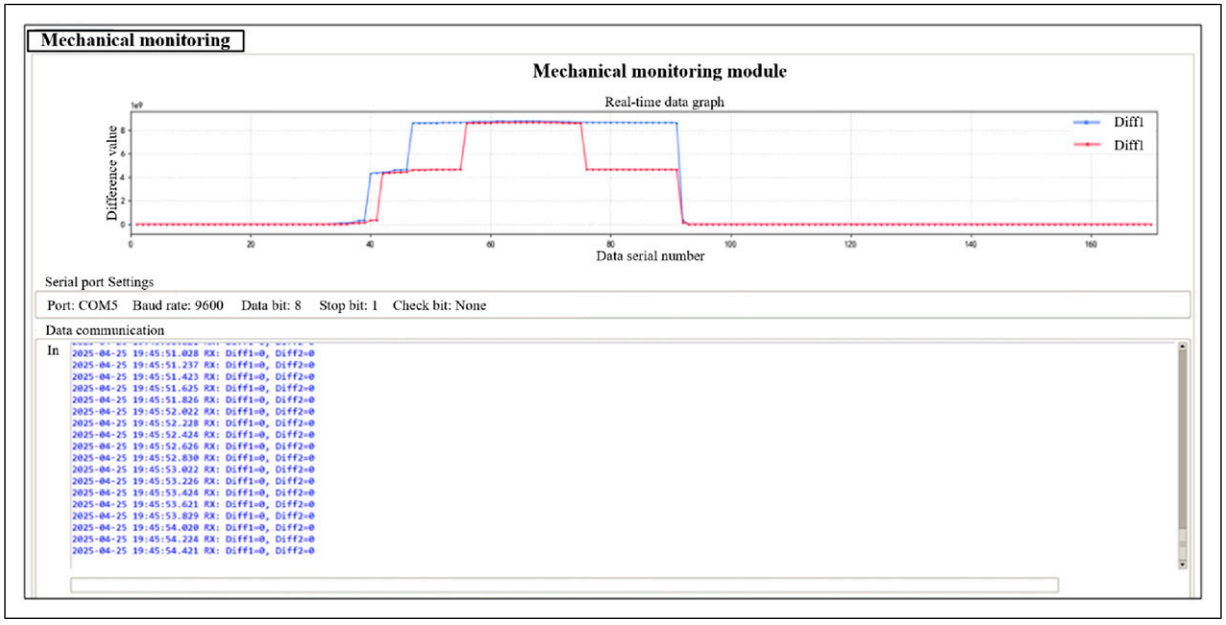

Figure 19. Real-time data display interface of the mechanics monitoring module.

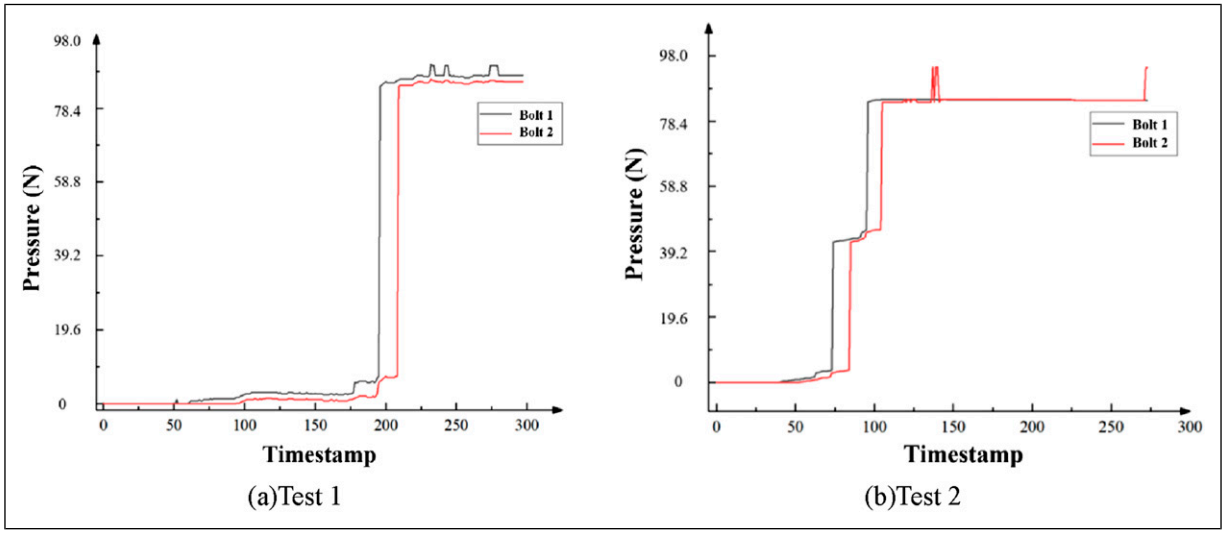

Figure 20. Bolt preload as a function of applied Torque. (a) Test 1. (b) Test 2.

smoothness of the loading curve. The pressure sensor output values for Bolt 1 and Bolt 2 at two monitoring points are recorded during the simulated bolt torque application. Both subplots clearly demonstrate that the monitoring device can capture the entire process in real time-from the initial relaxed state of the bolt, through torque application, to the final stabilization plateau. The resulting pressure plateau indicates that the device can reliably measure the bolt preload under static or quasi-static conditions, validating its measurement stability. Throughout both tests, data from the two monitoring points were continuously recorded, producing complete pressure variation curves. This confirms that the wireless communication link between the smart washer and the data receiver is fundamentally smooth and reliable, with no significant data loss, demonstrating good data transmission continuity and integrity under the experimental conditions.

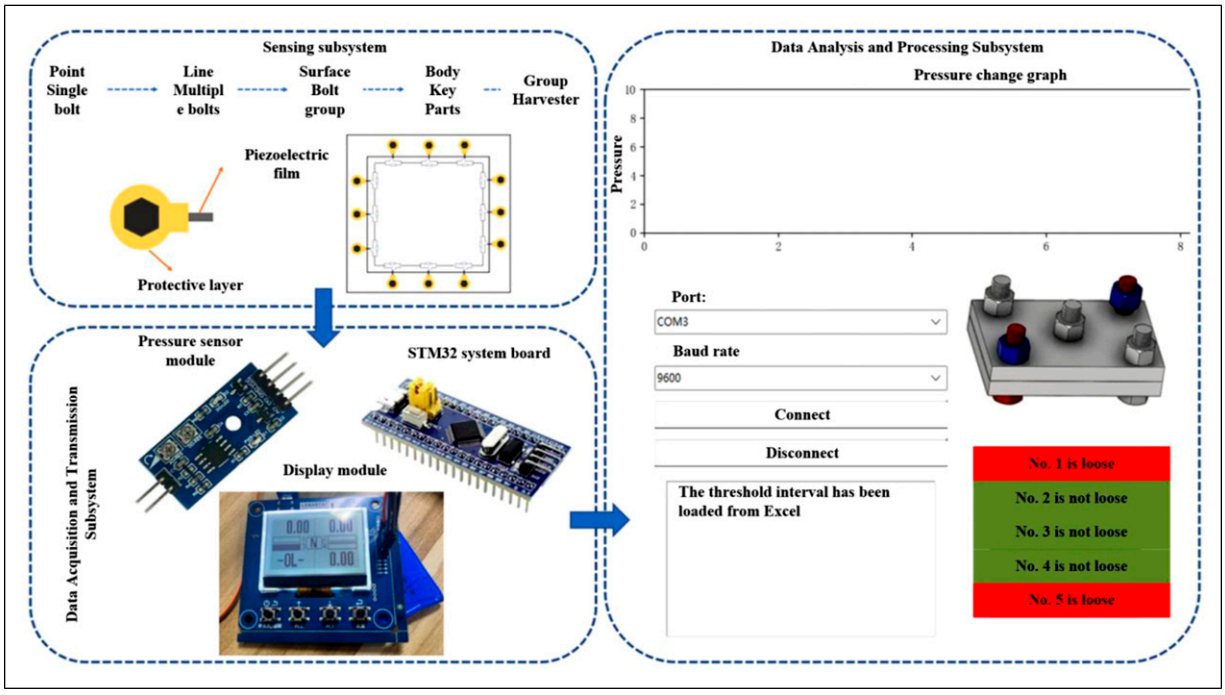

Figure 21. Bolt group loosening monitoring system for a combine harvester.

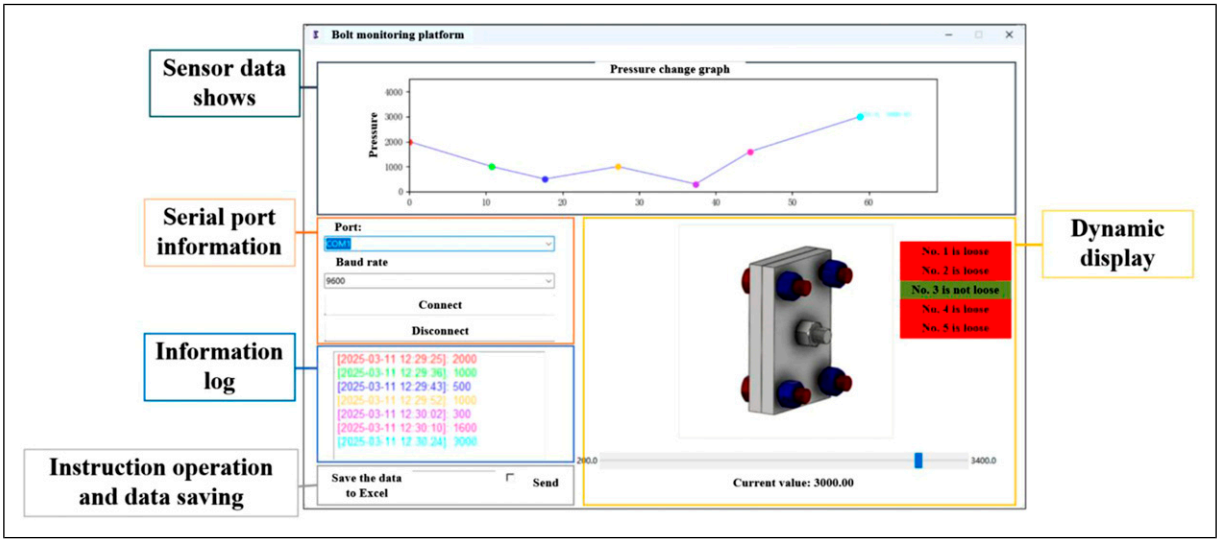

Figure 22. Man-machine interface architecture of multi-module pressure real-time monitoring and data management system based on serial communication.

3.4 Overall composition of the bolt loosening monitoring system

To effectively monitor the bolt connections of key components and the entire combine harvester, this study designed and built a monitoring system as shown in Figure 21. The bolt monitoring platform was developed using Python, enabling real-time and precise monitoring of bolt pressure states. Based on serial communication principles, configurable baud rates such as 9600 bps, 19200 bps, and up to 115200 bps are set to receive data streams from pressure sensors.

The software converts analog signals into pressure values and stores them in system documents. These data are dynamically visualized using real-time updated line charts that display subtle pressure changes over time. Simultaneously, a GIF animation player is driven to seamlessly switch between different bolt states-from tightened to loosened-based on preset pressure threshold ranges.

The software can send commands to the sensor devices for parameter configuration or data requests. Moreover, all received and sent serial port data, including timestamps and raw data, can be conveniently saved as Excel files for detailed subsequent data analysis, trend tracking, and long-term status recording. This provides a comprehensive and intuitive monitoring approach for bolt health management and maintenance.

(1) Sensing Subsystem: The piezoresistive loosening monitoring device designed in this study serves as the fundamental component of the entire system. Each device functions as a basic sensing node. Collectively, these nodes form a sensor network structured across five hierarchical levels, covering points, lines, surfaces, volumes, and groups. Each monitoring node can operate independently to fulfill monitoring tasks, while also enabling coordinated operation under a distributed cluster deployment.
(2) Data Acquisition Subsystem: This subsystem employs a microcontroller unit (MCU) to collect and store data. The data acquisition subsystem is a critical part of the monitoring device, with its core functionality implemented by the MCU. The MCU executes preset programs to periodically or event-triggeredly read analog signals from the piezoresistive sensors. After necessary signal conditioning, these analog signals are digitized by an internal or external analog-to-digital converter within the MCU. The resulting digital values represent the resistance changes related to bolt loosening states and are subsequently stored in designated storage media.
(3) Data Analysis Subsystem: This subsystem includes a specially designed data analysis interface for processing and analyzing data from the piezoresistive loosening monitoring devices, providing robust support for monitoring data analysis, as illustrated in Figure 22.

4. Conclusion

This study focused on the issue of bolt loosening in key components of combine harvesters and designed and validated a monitoring system with rapid detection and trend early-warning capabilities. The main conclusions are as follows:

1. A rapid detection method for bolt group loosening based on resistance encoding and regional binary search is proposed. Addressing the inefficiency of traditional individual inspection, this study innovatively designed a series resistance monitoring circuit, achieving unique decoding and localization of loosened bolts through changes in total resistance. Experimental results demonstrate that this method improves detection efficiency by up to 91.7% under multi-bolt conditions compared to traditional methods. By operationalizing efficiency strictly as the reduction in physical inspection steps, the results confirm that the proposed system optimizes the inspection workflow. The actual impacts on maintenance time, economic cost, and long-term field reliability remain to be quantitatively evaluated in future field studies.
2. A high-precision bolt pressure trend prediction model based on a feedforward neural network is constructed. To facilitate the transition from passive maintenance to predictive maintenance, the study employed a dual-hidden-layer structure combined with the Levenberg-Marquardt optimization algorithm to train the neural network. Test results show that the model accurately fits the decay trend of bolt clamping force, controlling the pressure prediction error for key bolts such as No. 9 and No. 10 to within 5%, thereby verifying its effectiveness in early warning.
3. An intelligent monitoring washer and visualization system integrating self-powering and long-distance communication capabilities is developed. Intelligent hardware integrating a miniature solar panel, LoRa wireless transmission, and piezoresistive sensing was developed, along with a corresponding Python-based real-time monitoring platform. The system achieves a closed loop from data acquisition and trend analysis to fault alarming, providing a robust and sustainable engineering solution for the bolt health management of complex electromechanical systems such as combine harvesters.

Although the proposed smart washer system has demonstrated excellent detection accuracy and application potential under controlled laboratory conditions, several critical limitations and challenges must be addressed prior to its large-scale industrial deployment on agricultural machinery (Figure 22). First, prolonged dynamic loading and high-frequency cyclic vibrations can easily induce mechanical fatigue and performance degradation in piezoresistive materials. Meanwhile, extreme temperature and humidity fluctuations may trigger sensor drift, and agricultural dust combined with harsh environments could compromise overall hardware stability. At the circuit and communication levels, the finite operational lifetime of relays and switches within the resistance encoding circuit may be severely shortened under high-frequency switching or adverse working conditions. Additionally, the power stability of miniature solar panels is susceptible to interference from dust accumulation and weather variations, whereas LoRa communication may suffer from signal attenuation and electromagnetic interference within electromechanical systems characterized by dense metallic structures. Furthermore, while the regional binary search mechanism is currently optimized for medium-sized arrays, its scalability to significantly larger bolt groups could be constrained by increased wiring complexity and potential signal-to-noise ratio (SNR) degradation in extended series circuits. Consequently, future work will focus on upgrading the sensor packaging to industrial IP67 standards for enhanced dust and moisture resistance, developing robust temperature compensation algorithms to suppress environmental interference, and conducting long-term vibration and loading trials on actual combine harvesters to comprehensively validate the system's reliability and durability under complex field environments.

ORCID iD

Jianpeng Jing https://orcid.org/0009-0000-0298-5964

Funding

The authors disclosed receipt of the following financial support for the research, authorship, and/or publication of this article: This research work was supported by the Inner Mongolia Autonomous Region Science and Technology Plan Project (2025YFDZ0033); the College Student Innovation Practice Fund of the School of Artificial Intelligence and Intelligent Manufacturing, Jiangsu University (RZCX2024001); and the Jiangsu Province University Students Practical Innovation Training Program Project (202410299060Z).

Declaration of conflicting interests

The authors declared no potential conflicts of interest with respect to the research, authorship, and/or publication of this article.

Data Availability Statement

The data used to support the findings of this study are available from the corresponding author upon request.

References

1. Liu N, Zhang W, Liu F, et al. Development of a Crop Spectral Reflectance Sensor. *Agronomy-Basel* 2022; 12: 2139, Article. https://doi.org/10.3390/agronomy12092139
2. Liu Y, Li Y, Ji K, et al. Development of a hydraulic variable-diameter threshing drum control system for combine harvester part I: Adaptive monitoring method. *Biosystems Engineering* 2025; 250: 174–182, Article. https://doi.org/10.1016/j.biosystemseng.2025.01.001
3. Ma Z, Zhang Z, Zhang Z, et al. Durable Testing and Analysis of a Cleaning Sieve Based on Vibration and Strain Signals. *Agriculture-Basel* 2023; 13: 2232, Article. https://doi.org/10.3390/agriculture13122232
4. Dai S, Wang M, Ou M, et al. Development and Experiment of an Online Measuring System for Spray Deposition. *Agriculture-Basel* 2022; 12: 1195, Article. https://doi.org/10.3390/agriculture12081195
5. Jin M, Zhao Z, Chen S, et al. Improved piezoelectric grain cleaning loss sensor based on adaptive neuro-fuzzy inference system. *Precision Agriculture* 2022; 23: 1174–1188, Article. https://doi.org/10.1007/s11119-022-09879-2
6. Tong Z, Zhang S, Yu J, et al. A Hybrid Prediction Model for CatBoost Tomato Transpiration Rate Based on Feature Extraction. *Agronomy-Basel* 2023; 13: 2371, Article. https://doi.org/10.3390/agronomy13092371
7. Bastek JH and Kochmann DM. Inverse design of nonlinear mechanical metamaterials via video denoising diffusion models. *Nature Machine Intelligence* 2023; 5: 1466–1475. https://doi.org/10.1038/s42256-023-00762-x
8. Gao Y, Yang Y, Fu S, et al. Analysis of Vibration Characteristics of Tractor-Rotary Cultivator Combination Based on Time Domain and Frequency Domain. *Agriculture-Basel* 2024; 14: 1139, Article. https://doi.org/10.3390/agriculture14071139
9. Rodriguez-Mier P, Garrido-Rodriguez M, Gabor A, et al. Unifying multi-sample network inference from prior knowledge and omics data with CORNETO. *Nature Machine Intelligence* 2025; 7: 1168–1186. https://doi.org/10.1038/s42256-025-01069-9
10. Sloane M, Solano-Kamaiko IR, Yuan J, et al. Introducing contextual transparency for automated decision systems. *Nature Machine Intelligence* 2023; 5: 187–195. https://doi.org/10.1038/s42256-023-00623-7
11. Wu J, Han BL, Zhang YH, et al. Enhancing Bolt Object Detection via AIGC-Driven Data Augmentation for Automated Construction Inspection. *Buildings* 2025; 15: 819. https://doi.org/10.3390/buildings15050819
12. Li SY, Le YS, Gao JC, et al. Bolt loosening angle measurement along full range of screw exposure length based on 3D point cloud. *Automation in Construction* 2024; 168: 105785. https://doi.org/10.1016/j.autcon.2024.105785
13. Han J, Yan X and Tang H. Method of controlling tillage depth for agricultural tractors considering engine load characteristics. *Biosystems Engineering* 2023; 227: 95–106, Article. https://doi.org/10.1016/j.biosystemseng.2023.01.011
14. Ma CD, Li AM, Du YL, et al. Efficient and scalable reinforcement learning for large-scale network control. *Nature Machine Intelligence* 2024; 6. https://doi.org/10.1038/s42256-024-00879-7
15. Shen Y, Gao J and Jin Z. Research on Acoustic Signal Identification Mechanism and Denoising Methods of Combine Harvesting Loss. *Agronomy-Basel* 2024; 14: 1816, Article. https://doi.org/10.3390/agronomy14081816
16. Jin Y, Liu J, Xu Z, et al. Development status and trend of agricultural robot technology. *International Journal of Agricultural and Biological Engineering* 2021; 14: 1–19, Article. https://doi.org/10.25165/j.ijabe.20211404.6821
17. Zhang B, Bai T, Wu G, et al. Fatigue Analysis of Shovel Body Based on Tractor Subsoiling Operation Measured Data. *Agriculture-Basel* 2024; 14: 1604, Article. https://doi.org/10.3390/agriculture14091604
18. Zhang Y, Zhao Z, Li X, et al. Near-Infrared-Based Measurement Method of Mass Flow Rate in Grain Vibration Feeding System. *Agriculture-Basel* 2024; 14: 1476, Article. https://doi.org/10.3390/agriculture14091476
19. Li D, Wang Z, Liang Z, et al. Analyzing Rice Grain Collision Behavior and Monitoring Mathematical Model Development for Grain Loss Sensors. *Agriculture-Basel* 2022; 12: 839, Article. https://doi.org/10.3390/agriculture12060839
20. Taylor R and Amer Soc Mechanical E. Understanding Bolt Stress Behavior In Temperature Cycling Environments. *ASME Pressure Vessels and Piping Conference (PVP) on Re-Energizing the Pressure Vessels and Piping Community*. Proceedings of asme 2023 pressure vessels & piping conference, 2023, vol 2.
21. Wang W, Li P, Li G, et al. Monitoring Method on Bolt Looseness Degree of GIS Insulating Spacer Based on Ultrasonic Wave. *High Voltage Apparatus* 2024; 60: 111–119.
22. Yang S, Sun J, Gu X, et al. A Temperature-Corrected Ultrasonic Attenuation Model for Bolt Looseness Detection. *Ieee Transactions on Instrumentation and Measurement* 2025; 74: 1–12. https://doi.org/10.1109/tim.2025.3545714
23. Chen D, Huo L and Song G. EMI based multi-bolt looseness detection using series/parallel multi-sensing technique. *Smart Structures and Systems* 2020; 25: 423–432. https://doi.org/10.12989/sss.2020.25.4.423
24. Chen D, Li W, Dong Z, et al. Multi-bolt looseness monitoring using guided waves: a cross-correlation approach of the wavelet energy envelope. *Smart Materials and Structures* 2024; 33: 125019. https://doi.org/10.1088/1361-665X/ad8d24
25. Yu W, Wang T, Deng S, et al. Bolt Connection State Monitoring Method Based on Fiber Grating Bolt Loosening Angle Measurement. *Chinese Journal of Sensors and Actuators* 2023; 36: 549–554.

26. Zhang W, Wang T, Yu W, et al. FBG-Based Loosening Angle Measurement Sensor for Bolt Looseness Monitoring. *Ieee Sensors Journal* 2025; 25: 4254–4260. https://doi.org/10.1109/jsen.2024.3502622
27. Liu P, Wang X, Chen T, et al. Research on a percussion-based bolt looseness identification method based on phase feature and convolutional neural network. *Smart Materials and Structures* 2023; 32: 035010. https://doi.org/10.1088/1361-665X/acb4cb
28. Peng M, Jin Y, Jin W, et al. On Line Monitoring Device of Bolt Tightening Force Based on Improved Wave Energy Method. *Chinese Journal of Sensors and Actuators* 2020; 33: 1557–1563.
29. Na WS. A portable bolt-loosening detection system with piezoelectric-based nondestructive method and artificial neural networks. *Structural Health Monitoring-an International Journal* 2022; 21: 683–694. https://doi.org/10.1177/14759217211008619
30. Li SY, Le YS, Li X, et al. Bolt loosening angle detection through arrangement shape-independent perspective transformation and corner point extraction based on semantic segmentation results. *Structural Health Monitoring-an International Journal* 2025; 24: 761–777. https://doi.org/10.1177/14759217241246643
31. Du F, Wu S, Xing S, et al. Temperature compensation to guided wave-based monitoring of bolt loosening using an attention-based multi-task network. *Structural Health Monitoring-an International Journal* 2023; 22: 1893–1910. https://doi.org/10.1177/14759217221113443
32. Du F, Wu S, Xu C, et al. Electromechanical Impedance Temperature Compensation and Bolt Loosening Monitoring Based on Modified Unet and Multitask Learning. *Ieee Sensors Journal* 2023; 23: 4556–4567. https://doi.org/10.1109/jsen.2021.3132943
33. Hu M, Yue N and Groves RM. Loose bolt localization and torque prediction in a bolted joint using lamb waves and explainable artificial intelligence. *Structural Health Monitoring-an International Journal* 2025; 24: 693–713. https://doi.org/10.1177/14759217241241976
34. Li X-X, Li D, Ren W-X, et al. Loosening Identification of Multi-Bolt Connections Based on Wavelet Transform and ResNet-50 Convolutional Neural Network. *Sensors* 2022; 22: 6825. https://doi.org/10.3390/s22186825
35. Zhang M, Wang L and Tian X. Bolt Loosening State Monitoring Based On Inner Product Matrix And Convolutional Autoencoder. *Engineering Mechanics* 2022; 39: 222–231.

https://dspace.org/

Rapid localization and predictive monitoring of bolt loosening in complex electromechanical systems: Smart washer system based on neural networks

Tang, Zhong; Jing, Jianpeng; Tian, Liquan; Lao, Liyun; Yuan, Lulu ...

2026-07
Sage
https://doi.org/10.1177/00368504261466980
Tang Z, Jing J, Tian L, et al., (2026) Rapid localization and predictive monitoring of bolt loosening in complex electromechanical systems: Smart washer system based on neural networks. Science Progress, Volume 109, Issue 3, July-September 2026, Article number 00368504261466980

Downloaded from a DSpace repository. https://dspace.org/